#### **Review Article**

Tao Liu, Weimin Lyu, Zhicheng Li, Shengke Wang, Xing Wang, Jiaxin Jiang\*, and Xiaosong Jiang\*

## Recent progress on corrosion mechanisms of graphene-reinforced metal matrix composites

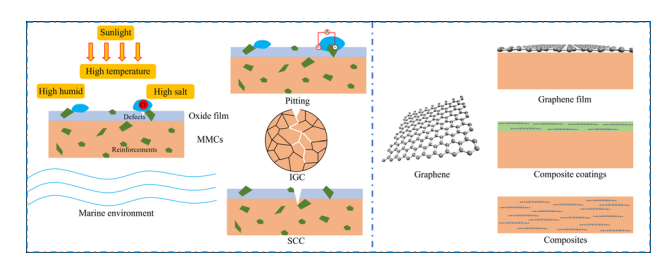
https://doi.org/10.1515/ntrev-2022-0566 received November 22, 2022; accepted June 6, 2023

**Abstract:** For components serving in high temperature, humidity, and salinity marine corrosive environment, it is vital to analyze the causes of corrosion behavior and corrosion mechanisms. Metal matrix composites (MMCs) are commonly used materials for offshore equipment. In this work, the corrosion factors of MMCs in marine environments are analyzed from the characteristics of high temperature, humidity, and salinity service environment, and the corrosion mechanisms are summarized. Graphene (Gr) has excellent comprehensive properties and great potential for applications in metal protection materials. In recent years, research into Gr anti-corrosive applications encompasses two aspects: pure Gr coatings and Gr composite coatings. Gr applied in MMCs is yet to be extensively studied. Therefore, this study analyzes the corrosion resistance of Gr-metal composites and discusses the corrosion resistance mechanisms of Gr-reinforced MMCs, which provides a reference for the design of Gr-reinforced metal composites and the optimization of corrosion resistance performance. Finally, future development directions for Gr-metal composites are proposed, and the critical factors such as defects, dispersion, content, size, arrangement, interface, and conductivity of Gr in the composites affecting their anti-corrosion properties are discussed.

**Keywords:** corrosion factors, corrosion mechanisms, graphene-reinforced metal matrix composites, marine corrosion, corrosion protection

**Tao Liu, Weimin Lyu, Zhicheng Li, Shengke Wang:** Naval Aeronautical University, Yantai, Shandong 264001, China

**Xing Wang:** School of Materials Science and Engineering, Southwest Jiaotong University, Chengdu Sichuan 610031, China



**Graphical abstract** 

#### 1 Introduction

Metals have been widely used in marine environments because of their excellent mechanical properties. Still, high humidity, high temperature, and high salt marine environment will cause significant harm to engineering equipment and facilities. Many inorganic salt ions (Cl-,  $Br^{-}$ ,  $S^{2-}$ , and  $SO_4^{2-}$ ) in seawater will deliquescence on the metal surface to form water films in high humidity. Han et al. [1] reported that Cl could accelerate the corrosion rate of composites. The oxide film will be destroyed by Cl-, thus promoting corrosion. Francis and Hebdon [2] also pointed out that as a highly conductive medium, the high galvanic current of seawater may accelerate the local dissolution of metals, thus leading to stress corrosion, pitting corrosion, crevice corrosion, and hydrogen embrittlement [3]. Metals are usually directly exposed to sunlight. The high temperature and light can accelerate the corrosion rate of metals, causing premature failure of metals. The economic loss caused by corrosion is approximately \$2.5 trillion (3.4% of the world's gross domestic product) annually reported by the National Society of Corrosion Engineers [4]. The annual loss of metals due to corrosion in various industries and service fields exceeds 10% of their yearly output [5]. Therefore, it is essential to study the corrosion mechanisms and choose appropriate ways to ameliorate the corrosion properties of metals according to the specific situation. To reduce the corrosion of metal materials, methods such as metal matrix improvement, cathodic protection, coating protection, and corrosion inhibitors can be adopted [13,15,17].

Due to their excellent performance, metal matrix composites (MMCs) are increasingly used in marine environments. The addition of reinforcements will not only improve the

<sup>\*</sup> Corresponding author: Jiaxin Jiang, School of Intelligent Manufacturing and Equipment, Chengdu Textile College, Chengdu 611731, China, e-mail: jiangjiaxin2004@126.com

<sup>\*</sup> Corresponding author: Xiaosong Jiang, School of Materials Science and Engineering, Southwest Jiaotong University, Chengdu Sichuan 610031, China, e-mail: xsjiang@swjtu.edu.cn

mechanical properties of MMCs, but also affect their microstructure, grains, precipitates, and internal defects, thus affecting the corrosion performance of the composites [1,6,7]. Li et al. [6] investigated the corrosion mechanisms of B<sub>4</sub>C/6061Al composites and reported that the corrosion pits on the surface mainly occurred at the interface of reinforcement/metal and the Sirich precipitated phase. Winkler and Flower [7] summarized the effects of reinforcements on the corrosion behavior of MMCs, mainly through the following: 1) Galvanic corrosion caused by the potential difference between matrix and reinforcements. 2) The selective corrosion of the interface of reinforcements/metal. 3) The corrosion of defects affecting the formation of intermetallic compounds. 4) There is almost no electrical reaction if the reinforcements are electrical insulators such as Al<sub>2</sub>O<sub>3</sub>, B<sub>4</sub>C, and SiC [7]. However, the interfacial reaction products bind the two materials together, and preferential corrosion may occur if the interfacial phase is a substantial anode or cathode. Shimizu et al. [8] studied the corrosion mechanisms of aluminum matrix composites, the corrosion potential  $E_{corr}$  of MMC is more susceptible to pitting due to the galvanic corrosion of the more potential reinforcement with the matrix. Although Al<sub>2</sub>O<sub>3</sub> and SiC fibers are non-conductive, their cathodic current is also more extensive than the matrix. Some phases would form at the reinforcement/matrix interface. Small pits were produced in all samples when the base metal and MMCs were immersed in 3.5% NaCl solution at room temperature for about a week. The pit growth on MMCs is faster than the alloy due to the dissolution of the matrix at the pit, forming a crack between the reinforcement and the matrix.

Among many reinforcements, graphene (Gr) has received attention due to its unique structure and excellent comprehensive properties [9]. Gr can act as a physical barrier layer to effectively block the passage of gas atoms such as water and oxygen [10,11]. Using Gr as a metal protective coating can prevent it from coming in contact with corrosive or oxidizing media and play a role in protecting the substrate material. However, galvanic corrosion tends to occur at the defect and interface [12]. Therefore, how to fully use the barrier effect to prepare defect-free Gr, insulating materials to encapsulate Gr, and Gr packaging strategies have attracted much attention. Sun et al. [13] proposed encapsulating rGO with APTES, which eliminated random connections in the matrix, thus inhibiting the corrosion activity of Gr. Gr can also play a passivation role in coating metal to improve its corrosion resistance [14,15]. Wang et al. [16] studied the influence of Gr addition on the corrosion behavior of Al/Al<sub>2</sub>O<sub>3</sub> composite coating and found that the small size effect of Gr could reduce the porosity. Due to the unique 2-dimensional structure, Gr can effectively isolate electrons and prevent the erosion of Cl in NaCl solution. In addition, the polymer coating commonly used in metal materials is easy to scratch, while the excellent tribological properties of Gr can improve the anti-wear and anti-friction properties of the material. Gr has been widely studied not only in composite coatings but also in enhancing the corrosion of metal substrates. Xie *et al.* [17] embedded exposed and semi-exposed graphene nanoplatelets (GNPs) into the oxide film and directly combined well with the oxide film with interface defects. Therefore, GNPs can act as corrosion inhibitors, reducing chloride entry and thus improving corrosion resistance. It is observed that GNPs and oxide film work together to form anticorrosive protective film through diffusion and chemical reaction. The doping of carbon atoms results in higher vacancy formation energy, Cl<sup>-</sup> entry energy barrier, and charge transfer work function.

This work reviews and summarizes the research progress on the corrosion mechanisms and protection of Gr-reinforced MMCs based on the influence of complex factors. First, the characteristics and influencing factors of environmental corrosion caused by high humidity, high temperature, and high salt service environment were summarized. Second, the corrosion types and mechanisms of high humidity, high temperature, and high salt are summarized in the service environment. Third, the anti-corrosion mechanisms of Gr composite designed according to the characteristics of Gr composite are summarized. On this basis, prospects of Gr-reinforced composites based on the influence of complex factors in the field of corrosion protection in metal materials are presented to improve their corrosion protection effect further and prolong their service life.

# 2 MMCs marine environment corrosion factors and corrosion mechanisms

Seawater has various gases dissolved in it and contains a lot of salts, which is a very harsh corrosive environment for various metal structures of marine engineering equipment. In the marine environment, the main factor for the accelerated corrosion rate of MMCs is the high Cl<sup>-</sup> content in the environment. Due to the harsh conditions of high humidity, temperature, and salinity in the marine environment, chloride salt will form on the metal surface after continuous moisture absorption and evaporation [18]. In high humidity and temperature, an electrolyte solution layer containing a high concentration of Cl<sup>-</sup> is formed on the surface. The solution contacts the substrate through the porous surface oxide layer and includes an oxygen concentration difference cell due to the difference in

concentration of Cl<sup>-</sup> distribution, causing electrochemical corrosion [41,42].

There are many influencing factors in seawater with different characteristics from other environments:

- 1) Seawater solution is close to neutral, shallow areas with more dissolved oxygen and oxygen depolarization process controls the corrosion of most metal materials in seawater, high concentration of Cl in seawater, even stainless steel (SS), can cause corrosion damage;
- The resistance of seawater is minimal, it is a fine conductive medium, and the contact between different kinds of materials could lead to galvanic corrosion, which may cause significant damage [18].

Metal structures often suffer localized corrosion damage, such as crevice and pitting corrosion. There are differences in the composition and concentration of seawater in different seas, and the effect of geographical factors is not essential [3]. However, water temperature, currents, and wind and waves vary greatly from sea to sea and influence the corrosion behavior of equipment and protection methods [2].

As shown in Figure 1, three main factors affect the corrosion of MMCs used in marine environments. Offshore engineering equipment has a complex structure and needs to withstand long-term use in harsh marine environments. Equipment under the marine environment's influence makes it easy to bring stress corrosion and other material safety issues [19]. Corrosion fatigue and wear significantly impact the safety of the structure in use [20-22]. In most cases, offshore construction equipment will be affected by multiple factors simultaneously, which can easily cause safety hazards and even disasters.

#### 2.1 Influencing factors of seawater corrosion

#### 2.1.1 High temperature factor induced material corrosion analysis

The temperature variation of seawater corrodes various materials to different degrees. In addition, temperature changes will lead to changes in other factors. For example, an elevated temperature increases the rate of oxygen diffusion, which in turn leads to an increment in the conductivity of seawater and an accelerated rate of corrosion. The temperature and its changes affect the marine atmospheric corrosion of metal materials by influencing the solubility of corrosive salts and gases in the water film, the condensation of water vapor on MMCs, the corrosion rate of the anode and cathode processes in the corrosion cell, and the resistance of the water film. In the marine atmosphere corrosion environment, the relative humidity (RH) is often higher than the critical RH of MMCs, temperature increases, and corrosion significantly accelerates. Neville and Hodgkiess [23]

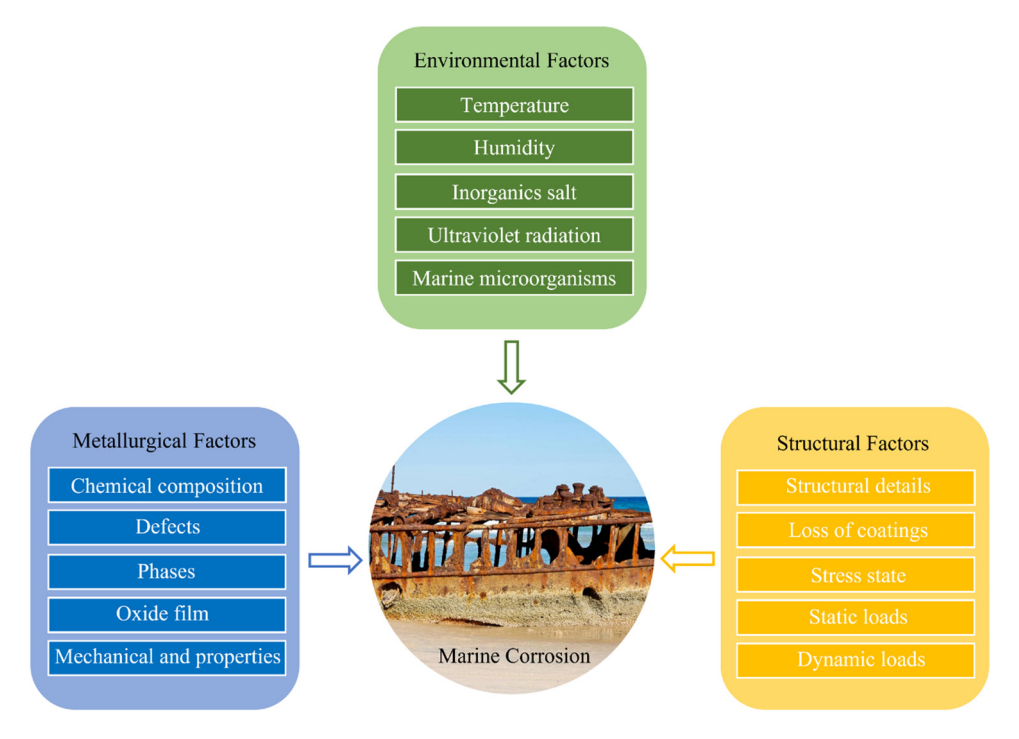


Figure 1: Factors affecting marine corrosion.

studied the effect of high-speed impingement flow and high temperature (60°C) on the corrosion behavior of SS and related nickel- and cobalt-based alloys in marine environments. He pointed out that the temperature increases significantly promoted the premature breakdown of the passivation of all materials. The effect of high-speed impingement flow was to further shift the breakdown potential of passivation to more positive values. With the increase in the temperature, the oxidation passivation film became thin and porous, and the protection was diminished due to the dissolution of the film [24]. In Zakaria's study [25], the corrosion performance of Al/SiC composites is positively correlated with temperature. The effect of temperature depends on the activation energy of corrosion. For MMCs, the corrosion rate increases with the activation energy and temperature increase. In the marine atmosphere, the temperature rise will promote the diffusion of corrosive chloride ions and oxygen, changing the relative content of main corrosion products and accelerating corrosion [44].

However, the influence of temperature is not a simple linear relationship [26]. The solubility of oxygen decreases with the increase in temperature, thus inhibiting metal corrosion [27]. Zhang studied the corrosion behavior of Cu–Al composites at 35, 45, and 55°C. The corrosion rate was the highest at 45°C. The Arrhenius formula analyzed the corrosion rate of Cu–Al composites at different temperatures.

$$\ln K = -\frac{E_{\rm R}}{RT} + B,\tag{1}$$

where K is the anodic reaction rate,  $E_R$  is the activation energy, T is the thermodynamic temperature, R is the molar gas constant, and B is the frequency factor. According to the formula, the increase in temperature leads to an increase in the K value, which accelerates the anode reaction. When the temperature increases to a certain extent, the oxygen content in the solution gradually decreases, leading to a decrease in the cathode reaction rate, thus inhibiting the reduction reaction. Flores  $et\ al.\ [28]$  evaluated the effect of temperature on the corrosion process of MMCs using Arrhenius diagrams. As shown in Figure 2, the corrosion rate of MMCs varies with temperature, and there is a

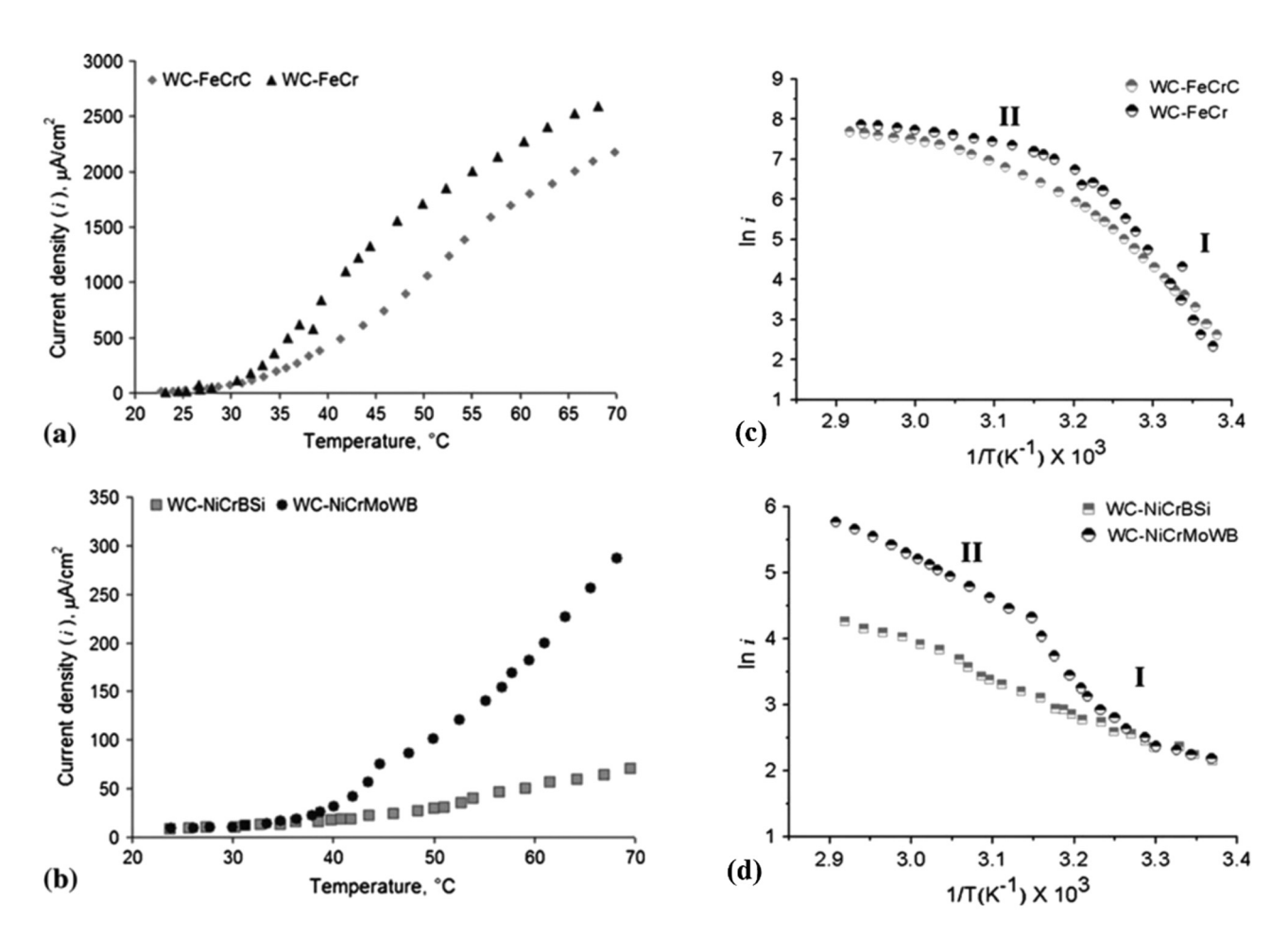


Figure 2: Current density (i) as a function of temperature for the MMCs: (a) WC-FeCrC and WC-FeCr MMCs and (b) WC-NiCrBSi and WC-NiCrMoWB MMCs; Arrhenius plot of the potentiostatic tests of the MMCs: (c) WC-FeCrC and WC-FeCr MMCs, and (d) WC-NiCrBSi and WC-NiCrMoWB MMC [28].

critical transition temperature  $T_{\rm c}$  for the corrosion rate. When the temperature is higher than  $T_c$ , the range of priority attack zone of MMCs increases, and the number of voids and "microcrack like" sites increase.

#### 2.1.2 High humidity induced material corrosion analysis

Corrosion in atmospheric environments is a discontinuous process that depends on the availability of electrolytes to provide ionic conduction between the cathode and anode. Pitting occurs when an aerosol of salt particles is deposited on MMCs, and the RH reaches the deliquescence point of salt [29]. The deliquescence RH (DRH) of NaCl, the main corrosion medium in the marine environment, is 76%. When the humidity exceeds DRH, solid NaCl will absorb water and deliquescence to form a solution. Schindelholz et al. [30] studied the influence of RH on steel corrosion. The deliquescence point of NaCl does not represent a critical RH value, and corrosion can continue even at 33% RH, as shown in Figure 2. The corrosion rate significantly increased when RH reached 53%, which was 20% lower than the DRH of NaCl. However, the considerable variation in attack between 33 and 53% is due to the chemical hygroscopic behavior formed at the anode and cathode. NaCl deliquescence point corrosion is caused by several physical phenomena under or maintained. These physical phenomena allow the existence of electrolytes, including:

- 1) The existence of the adsorbed water related to steel surface salt;
- 2) Crystallizing point inhibition caused by the existence of the supersaturated salt water;
- 3) The hygroscopicity of chemical corrosion.

Due to the relatively high RH in the ocean atmosphere, the RH of the air is higher than its critical value [31,32], so a thick corrosive water film will be formed. Steel's corrosion behavior and corrosion mechanism are directly affected by the thickness of the water film on the surface. The corrosion rate increases with the increase in water film thickness. The marine atmosphere corrosion process of corrosive water film on composite material is consistent with the law of electrochemical corrosion in electrolytes. In this process, it is especially easy for oxygen to reach the surface of composite materials, and the corrosion rate of composite materials is controlled by oxygen polarization. The critical RH for pit reactivation 304 is 70–75% and 56–70%. Thus, stable pits grown under invasive conditions will be blunted when RH changes to high values greater than 75%. When the RH of the metal is greater than 70%,

the corrosion is severe [33]. Although NaCl is the main component of sea salts, which has a tidal RH of about 76%, the presence of highly hygroscopic salts such as MgCl<sub>2</sub> (33% tidal RH) means that sea salt particles begin to wet much earlier [34]. In Cheng et al.'s study [35], the corrosion rate of zinc metal increased with the increase in humidity, with the highest corrosion rate at 97%. Anodic and cathodic processes determine the corrosion rate, and RH mainly affects the cathodic process. The polarization curves of different humidity (75, 85, and 95%) in Huang et al.'s study [36] showed that the initial corrosion process was controlled by oxygen reduction, and the corrosion rate increased with humidity. However, when exposed for a long time, the corrosion products increased with higher RH, which inhibited the anode's dissolution and decreased the corrosion rate. Wang et al. [37] used an electrolytic method to prepare superhydrophobic zinc-dodecane complex film on a zinc surface, and the obtained film can maintain superhydrophobic properties in the solution system and effectively inhibit corrosion. However, in the simulated marine environment, salt water penetrates the superhydrophobic film during the deliquescence process of NaCl particles, which weakens the advantage of the superhydrophobic film as a corrosion barrier of the marine atmosphere (Figure 3).

#### 2.1.3 High salt induced material corrosion analysis

The marine environment is highly corrosive due to large amounts of salt substances. Among these salts, chlorine salts and sulfates are prone to corrosion, while chlorine salts account for a considerable proportion of seawater and mainly cause changes in the conductivity of seawater [38]. The salt particle impurities dissolve in the water film, becoming a highly corrosive electrolyte and accelerating corrosion. In addition, due to the good hygroscopic property of Cl<sup>-</sup> and the relatively high humidity of the ocean atmosphere, other Cl droplets are easy to form in the interface between dry and wet sea water and adhere to the metal surface [39]. Ambler and Bain proved that when the thickness of Cl containing droplets deposited on the metal surface exceeds 10 µm, corrosion will be caused [40]. In marine environments, chloride deposit on the metal surface to form a thin layer of liquid electrolyte and become the critical factor influencing the marine structures metal. Frankel's [41] polarization test method proves that the metal corrosion rate increases with the increased concentration of Cl<sup>-</sup>, and the pitting potential of metal is a linear function of the logarithm of Cl<sup>-</sup> concentration.

— Tao Liu et al. DE GRUYTER

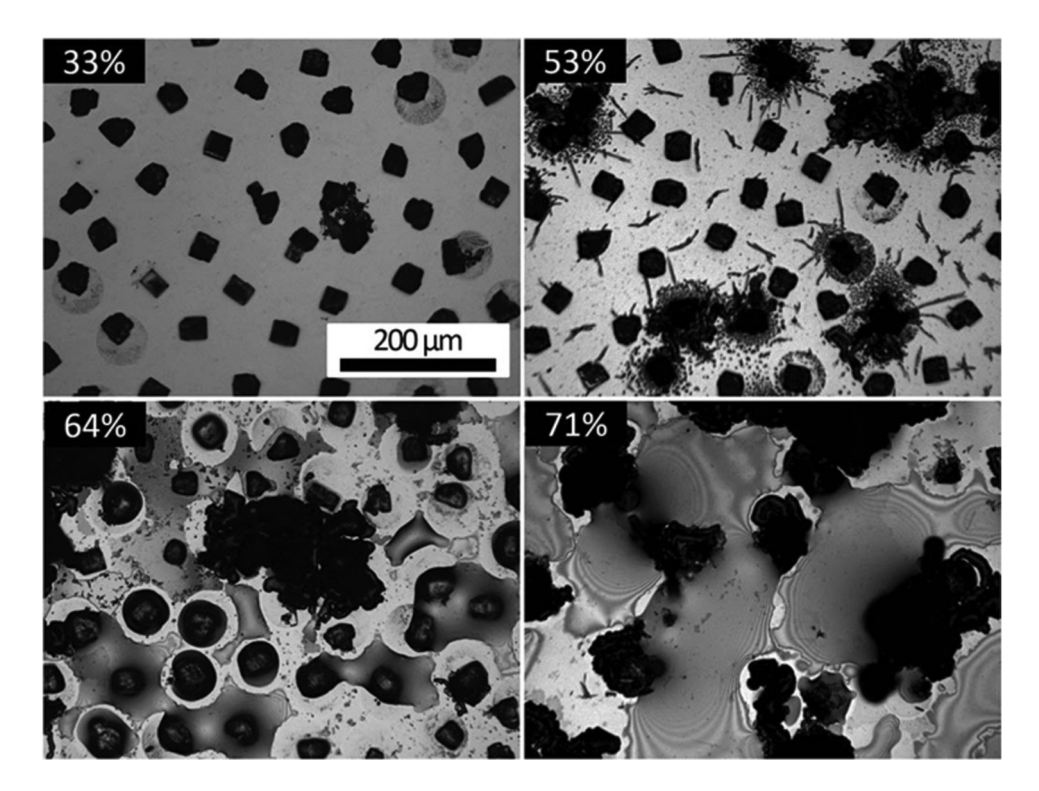


Figure 3: Optical micrographs of crystal-loaded coupons immediately after 7 days of exposure below the DRH of NaCl. The RH was controlled at the indicated value during the imaging. The black regions are rust formation and electrolyte pools are readily visible in the 64 and 71% images [30].

The salinity of seawater will directly affect the content of oxygen and electrical conductivity of seawater, which will change with the increase in the salinity of seawater, affecting the corrosion of materials. Moreover, the corrosion rate of seawater will reach a maximum value with different salinity. The higher the chloride concentration, the more severe the corrosion. When NaCl concentration was lower than 3 wt%, the increasing weight loss trend was more obvious than when NaCl concentration was higher than 3 wt% [26]. The higher the chloride concentration, the higher the corrosion current density. The chloride solution quickly reaches the anode limit current density in the anode region. In the cathode region, the self-corrosion current density of the solution containing chloride ions decreases, and chloride ions have a certain inhibitory effect on the cathodic reaction. Among the many factors of marine corrosion, chloride concentration has the greatest impact on the corrosion rate of metal materials. However, the chloride concentration changes due to the ocean's different regions and the water film's evaporation. Li et al. [42] investigated the corrosion behavior of Cu-4Ti alloys in simulated contaminated seawater (3.5 wt% NaCl solution containing S<sup>2-</sup>. The S<sup>2-</sup> and Cl<sup>-</sup> have competing adsorption effects on the corrosion of Cu–Ti alloy, and the strong adsorption of S<sup>2-</sup> causes severe corrosion of Cu-Ti alloy.

#### 2.1.4 Complex factor induced MMCs corrosion analysis

Actual seawater corrosion is often multi-factor coupled, which has a certain difference compared to the existing corrosion behavior of materials under single-factor conditions and the corrosion mechanism.

#### 2.1.4.1 Dry and wet alternation

Few researchers studied the corrosion behavior and mechanism of MMCs under alternating wetting and drying. Still, it is an unavoidable problem to explore the corrosion mechanism of MMCs in the alternating wetting and drying environment. This study summarizes metal materials' related mechanisms and research progress in wet and dry alternations. The surface of metal materials is often in a state of alternating wetting and drying under the oceanic atmosphere, which will lead to a high concentration of salt on MMCs and thus affect the corrosion rate of metal materials [43]. The air's RH affects the wetting and drying frequency by affecting the water film's thickness. If the sunshine time is too long, the water film will disappear, reducing the wetting time of the surface and the total amount of corrosion. In addition, rain and wind speeds also affect the alternating frequency of wet and dry film on metal surfaces. Some scholars measured the instantaneous corrosion rate of nickel-containing steel by continuous measurement of polarization resistance and found that the wet period of the metal surface was determined by high-frequency impedance. The oceanic and atmospheric environment contains a large amount of Cl<sup>-</sup>, and the changes after the second stage of atmospheric corrosion are influenced by Cl<sup>-</sup>, forming aqueous hydrous hydroxide [44].

Various forms of corrosion failure of MMCs occur in marine environments. Liang et al. [45] investigated the corrosion behavior of 6060 aluminum alloys in the ocean tidal, splash, and immersion zones, respectively. The results show that the most intense and dense pitting corrosion occurred in the submerged area. The corrosion forms include shallow pit and deep pit, intergranular corrosion (IGC), and crystal corrosion. This is the result of accumulated corrosion products under local hypoxia conditions. However, corrosion in the tidal and splash zones was less severe. Bailey and Li [46] simulated the wetting process of splashing and the subsequent drying process of exposure to weather. In the study of the dry-wet cycle, it was found that samples under the dry-wet cycle had significant pitting erosion compared with samples under continuous immersion.

#### 2.1.4.2 Light conditions

Light condition is an essential factor affecting marine atmospheric corrosion of materials. Light can promote the photosensitive corrosion reaction of iron metal surfaces and the biological activity of fungi, which provides a greater possibility for moisture and dust to be stored and corroded on metal surfaces [47]. Lin and Frankel's study [48] proved that ultraviolet light can accelerate the corrosion of copper. The effect of light is manifested in two aspects: first, corrosion products formed on the surface, such as Cu<sub>2</sub>O, CuO, ZnO, FeO, FeOOH, and Fe<sub>2</sub>O<sub>3</sub>, mostly have the properties of semiconductors. Under light radiation, a photovoltaic effect will be generated, and electrons and holes will be formed, changing the charge distribution state. To accelerate or inhibit the corrosion process [49]. Electrons are excited from the valence band (VB) into the conduction band (CB), leaving holes when illuminated by external light of the appropriate wavelength. Photogenerated electrons can reduce, and photogenerated holes can oxidize. The photogenerated electrons can participate in the chemical reaction and affect the corrosion process. Second, light can affect the cathodic and anodic process of corrosion reaction by affecting the thickness of electrolytic thin liquid film on metal surfaces [50]. Song and Chen [51] reported that UV illumination significantly increased the rate of NaCl-induced atmospheric corrosion of zinc.

The positive photovoltage after exposure to corroded zinc was observed under illumination, indicating that the influence of ultraviolet irradiation on the atmospheric corrosion of zinc is mainly through the photovoltaic effect of corrosion products with semiconductor properties. Chen et al. [52] found that ultraviolet irradiation decomposed molecular oxygen into atomic oxygen. Atomic oxygen can participate in the oxidation of silver. Li and Li [53] studied the photoelectric chemical anticorrosion effect of the corrosion product layer of electro-galvanized steel in simulated seawater and concluded that the oxide and corrosion product layer could not only withstand the erosion of harsh environment but also provide additional photocathodic protection for electro-galvanized steel under simulated sunlight. The steel corrosion product layer's corrosion protection effect under light conditions is 30% better than that under dark conditions. Photoelectrons generated by the ZnO layer can transfer to the substrate to provide cathodic protection for electro-galvanized steel under sunlight. UV illumination affects the formation, morphology, and properties of corrosion products. In Song et al.'s study [54], the electrical conductivity of corrosion products of weathering steel under UV light was much higher than that after exposure to the dark. The increase in electrical conductivity will enhance the carrier strength of the corrosion product layer, increasing chemical reactivity. The formation of Fe<sub>3</sub>O<sub>4</sub> and reduction of y-FeOOH were promoted by UV irradiation. The corrosion product layer formed under ultraviolet irradiation has photoelectric rectification characteristics similar to N-type semiconductors. Reduction of y-FeOOH occurs mainly in ultraviolet light, where the photovoltaic effect excites electrons in the VB into the CB, thus leaving holes in VB. Γ-FeOOH quickly captures photogenerated electrons. y-FeOOH is present in the corrosion product layer and can be used as an effective oxidant in the subsequent reduction reaction.

#### 2.1.4.3 Marine microorganisms

The corrosion of materials by marine organisms has two sides. The effect of slowing down the corrosion of materials can be effectively prevented by the diffusion of dissolved oxygen to the material surface if the attached marine organisms are continuous and tightly packed. Conversely, for SS and other easily passivated metals, the corrosion will be aggravated if the attached marine organisms are intermittent or uneven, resulting in local anoxia forming oxygen concentration differences and local corrosion of the occluded cell type. Various types of carbon steel and SS widely used on the hull of ships are subject to corrosion by several types of microorganisms to varying degrees and failure [55,56].

Xu et al. [57] investigated the influence of marine aerobic biofilm on the corrosion of 316L SS in aeration and deaeration seawater. The aerobic biofilm inhibited the corrosion of 316L SS during the test period. A comparison of the results under aeration and deaeration conditions indicated that the aerobic biofilm inhibited the corrosion of 316L SS requiring live cells, and the polarization curves indicated that the biofilm mainly inhibited the anodic effect. The current–potential curves under deoxygenation conditions showed an electron transfer process between the microorganism and the electrode, as shown in Figure 4.

### 2.2 MMCs corrosion mechanisms in the marine environment

After long-term research, the corrosion process of MMCs is complex, but in essence, they go through two completely different processes: pure chemical and electrochemical. No matter how the corrosion reaction process is, electron transfer will occur when corrosion occurs, and the electron transfer will inevitably lead to the fracture of old bonds and the generation of new bonds. The corrosion of MMCs in the marine environment is mainly electrochemical corrosion. Under the influence of many factors in the marine environment, a protective layer composed of oxides and hydroxides is formed on the surface of the MMCs in the initial stage. In a high salt and humidity marine environment, the electrolyte is formed on the surface owing to water adsorption and precipitation of corrosive gases and solid salt particles. For MMCs, the pores and other defects on the surface will form a water film due to the capillary effect. Schindelholz et al.'s [30] research shows

that water first adsorbs on metal surface defects to form electrolytic cells. In different MMCs, pitting always occurs at the surface defects. Due to the addition of reinforcement in MMCs, there will be defects at the reinforcement/metal interface. When the electrolyte is formed at the defect of the interface, galvanic corrosion will be formed because of the potential difference between the reinforcement and the metal matrix. The potential of the reinforcement may be higher or lower than that of the matrix, or it may change in corrosion. When the corrosion potential of reinforcement is higher than that of the matrix, the reinforcement will act as an anode and cause the dissolution of the metal.

The thickness of the water film on the metal surface will also increase in a higher RH environment. The corrosion rate increases sharply because of the increase in the conductivity of the electrolyte, then decreases slightly because of a decrease in the rate of oxygen diffusion to the metal surface. For MMCs with different substrates, the properties of the oxide film are also different. The introduction of reinforcement will inevitably affect the corrosion performance of composites while improving their mechanical properties and other properties. The corrosion resistance of MMCs depends on their corrosion potential and the properties of the oxide film. The corrosion behavior of Al composites and Mg matrix composites showed that Gr would reduce the corrosion resistance of the matrix. Rashad et al. [58] investigated the corrosion mechanisms of Mg/GNP composites in NaCl solution. An oxide film is formed after a reaction with an aqueous solution, and the film is composed of Mg, MgO, and Mg(OH)2. The corrosion first occurs in the matrix near the GNPs region, forming local pits and deepening with time. The fracture attack caused by the dislocation density at the composite interface leads to a higher corrosion rate than that of the

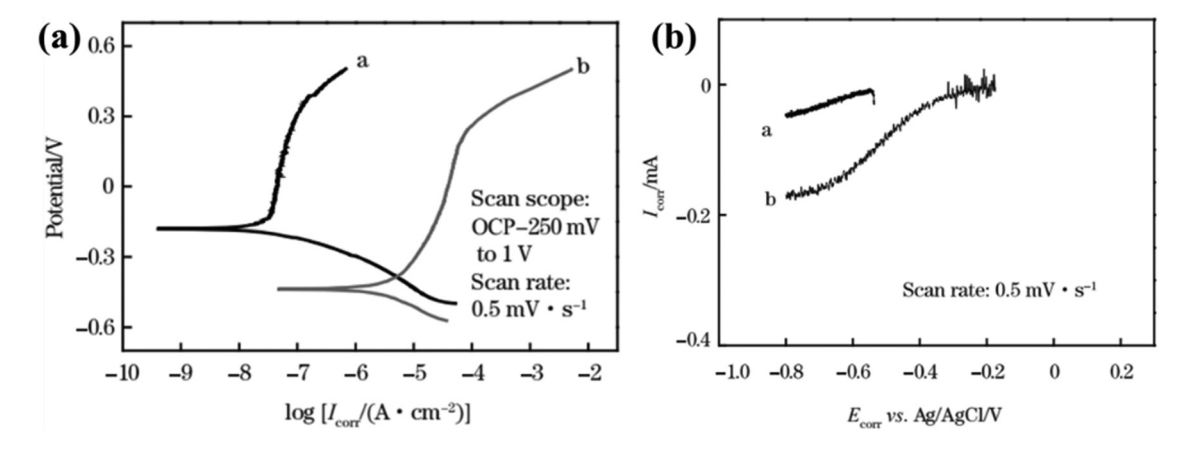


**Figure 4:** (a) Polarization plots of 316L SS after 6 days of immersion in natural and sterile seawater and (b) current–potential curves of 316L SS after 6 days of immersion in sterile and naturally deoxygenated seawater [56].

non-reinforced alloy. The pits are formed by anodic reactions that produce  $Mg^{2^+}$  that diffuse outward from the surface. Chloride ions migrate inward the pit to maintain electrical neutrality. With the progress of corrosion, the pit became larger and broader, which destroyed part of the protective film on the Mg matrix.

The locations near Gr that do not have GNP regions are also prone to pitting because of the interface's discontinuity of the protective oxidation-hydroxide layer. For Fe matrix composites, it is found that hydrogen is concentrated in the iron grain boundary, which makes Fe-Fe bonds parallel to the grain interface stronger than those perpendicular to the grain interface, so it is easy to produce intergranular fracture [59,60]. Hydrogen will change the state of α-Fe atoms, resulting in severe anisotropy of the strength of different cleavage planes in the crystal and significantly reduce the number of lattice electrons in the crystal, which may make α-Fe easy to fracture. The presence of Cr will accelerate the development of corrosion products to the thermodynamic steady state, namely, the transformation process of  $Fe_xH_yO_z \rightarrow y$ -FeOOH  $\rightarrow \alpha$ -FeOOH  $\rightarrow \alpha$ -Fe<sub>2</sub>O<sub>3</sub>. In Fe/(TiB<sub>2</sub>-CNT) composite coating, Liu *et al.* [61] confirmed that the presence of Cr could make the  $\alpha$ -FeOOH rust layer have cation selectivity, that is, preventing Cl<sup>-</sup> and  $SO_4^{2-}$  from penetrating the matrix surface, thus making the rust layer have a protective effect [62]. Chromium improves the solid solution's stainless iron base electrode potential and the absorption of electronic iron passivation to impel the contradiction movement of SS internal development to improve corrosion resistance. Therefore, with the increase in chromium content, the corrosion rate of steel decreases continuously. When the chromium mass fraction exceeds 12%, the steel is difficult to corrode and rust. Molybdenum promotes the passivation of Fe-Cr SS and enhances its corrosion resistance, especially the local corrosion resistance in chloride solution [63,64]. The interface between the reinforcements and Fe matrix will become the main starting point of pitting corrosion, and the galvanic corrosion also accelerates the corrosion of the composite because of the potential difference.

#### 2.2.1 Pitting mechanisms

Pitting corrosion is the main corrosion form of MMCs. Passivation film forms on the MMCs surface in a neutral aqueous solution without corrosive ions. However, the pitting of MMCs is enhanced when exposed to corrosive anions such as Cl<sup>-</sup> in high temperatures. Pitting corrosion occurs when isolated sites of MMCs suffer from rapid attack due to the local breakdown of protective passivity.

At the same time, most of the adjacent surfaces remain virtually unaffected, as shown in Table 1.

Sea water will priority adsorb at defects in MMCs. Aggressive anion could passivate the membrane on the surface to be delivered to the interface, where the formation of an electrolytic cell to start the role of the specific mechanism (through) [41], or adsorbed on the surface oxide, reinforced metal cations from oxide to transfer of the electrolyte. The film-breaking mechanism requires that the fracture be carried out within the membrane to allow the anion to directly enter the unprotected metal surface [65]. Once the pit begins to grow, the cathode reactants in the pit, for example, O<sub>2</sub>, are depleted, which transfers most of the cathodic reactions to the exposed

**Table 1:** Different types of realistic morphologies of pitting corrosion

Type of pitting	Morphologies of pitting
Narrow, deep	
Shallow, wide	
Subsurface	
Undercutting	
Vertical grain attack	WI)
Horizontal grain attack	=
Elliptical	

surface outside the pit, while the anodic reactions take place inside the pit. The anodic reaction products, metal cations, are enriched in the pit, and Cl<sup>-</sup> migrates to the pit to remain electrically neutral. The growth of the pit was facilitated by the hydrolysis of metal cations and the lower pH inside the pit than outside the pit. Ao et al. [66] studied the corrosion mechanisms of 6061Al/(TiC-Al<sub>2</sub>O<sub>3</sub>) composites. They found that the introduction of TiC-Al<sub>2</sub>O<sub>3</sub> of fine grain size, and the number of intermetallic compounds AlSiFe and AlMgSiCu increased at the grain boundary. Galvanic corrosion can be formed due to the potential difference between reinforcement, intermetallic compounds, and aluminum matrix. Al<sub>2</sub>O<sub>3</sub> does not participate in galvanic corrosion due to its insulation. The surface energy of the low exponential Miller plane shows that Cl<sup>-</sup> is readily adsorbed on the AlSiFe phase, which increases the concentration of Cl<sup>-</sup> and leads to the breakdown of the AlSiFe phase indicating the passivation film. Therefore, pitting occurs preferentially in AlSiFe.

In Ao et al.'s study [66], the electrical conductivity and insulation of the reinforcements are important influencing factors. Simultaneously, the intermetallic compounds produced by the reaction between the matrix and reinforcement will also affect the corrosion performance. The coupling between the metal matrix and reinforcement or the second phase causes the pitting of MMCs. Boag et al. [67] reported that the stable pit of AA2024-T3 aluminum alloy is usually located at intermetallic particles (IMPs). The formation of a stable pit in the alloy requires three steps: (1) Coupling: Al<sub>2</sub>CuMg (S phase) and Al matrix are coupled with Al-Cu-Fe-Mn IMPs. The Al-Cu-Fe-Mn IMPs act as the cathode to support the anodic dissolution of the Al matrix and S phase; (2) Pitting: Pitting occurs around imp, increasing the susceptibility to local corrosion. (3) Dealloying: after the S-phase is unalloyed owing to corrosion, it becomes a cathode, and Cu is re-deposited on the nearby Al-Cu-Fe-Mn IMPs, which improves its cathodic activity. Pitting occurs preferentially in these grains due to the high electrochemical activity of the T1 phase. Since the T1 phase tends to precipitate on the {111} plane, these sites are more susceptible to corrosion [68]. Pitting corrosion in aluminum alloys correlates with the second phase's quantity and distribution [69].

Pardo *et al.* [70] found two corrosion mechanisms in the research of the effect of SiC content and Al matrix composition of reinforcement on the corrosion behavior of the composites. At the beginning of corrosion, chloride ions lead to nucleation and growth of pits. Nucleation pits start at the  $\rm SiC_p/matrix$  and intermetallic/matrix interfaces. Dissolution is rapid in the pit, whereas aerobic reduction occurs on the adjacent surface. High concentrations of  $\rm H^+$  and  $\rm Al^{3^+}$  are produced in the pit due to cationic hydrolysis

 $(Al^{3+} + 3H_2O \rightarrow Al(OH)_3 + 3H^+)$ . At the later stage of corrosion, there is a significant hydration-induced growth of the Al<sub>2</sub>O<sub>3</sub>·3H<sub>2</sub>O porous layer, which reduces the corrosion rate. Longer immersion time or alternating cycles of low and high humidity are conducive to cracking the protective layer of corrosion products, thus promoting the penetration of oxygen, chlorine, and water. This facilitates the formation of an Al<sub>2</sub>O<sub>3</sub>·3H<sub>2</sub>O layer grown inside the material, resulting in a corrosion loss of Al because of the dissolution of metal and SiC/matrix interface pitting. The Cu-Al galvanic couple accelerated the degradation process. The intermetallic compound Al-Cu has a strong cathodic effect on the metal matrix and, as the cathodic site, promotes the dissolution of Al<sub>2</sub>O<sub>3</sub> and enhances the pitting corrosion. The existence of SiC<sub>p</sub> and Cu-Al galvanic couple is beneficial to the nucleation and growth of the corrosion layer.

Hu et al. [71] studied the corrosion mechanisms of Zr-Cu-Ni-Al metallic glass (MG) composite coatings and found that MG has high chemical activity, which makes the surface oxidize rapidly, leading to the increase in  $i_{corr}$ . The porosity can improve the self-corrosion current density in the coatings. In the polarization process [72], the metal elements are oxidized to Al2O3, NiO, ZrO2, and Cu<sub>2</sub>O. It is well known that Al<sub>2</sub>O<sub>3</sub>, NiO, and ZrO<sub>2</sub> are dense and usually exhibit stable chemical activity, while Cu<sub>2</sub>O is loose because of volume expansion in oxidation [73,74]. In the process of polarization, aggressive chloride ions preferentially adsorb on the interface and porous structure [75]. Therefore, porous Cu<sub>2</sub>O will become the preferred adsorption site for Cl<sup>-</sup>, and part of Cu<sub>2</sub>O will be converted to CuCl. Owing to the thin passivation layer, local adsorption of Cl<sup>-</sup> will promote the dissolution of Cu<sub>2</sub>O, leading to the pitting and thinning of the oxide film [76]. Cl can migrate through the surface film when pitting occurs and react with the metal, forming metal chloride on the metal/film surface [77]. The solubility of CuCl is low, but the formed CuCl will precipitate on the corroded surface, resulting in copper enrichment at the pitting site. Kinetically, CuCl is converted into Cu<sub>2</sub>O. The dissolution and chlorination of porous Cu2O may mainly cause the passivation damage of the Zr-Cu-Ni-Al coating. MG promotes the formation of a passivation layer with its high chemical activity and inhibits the formation of pitting by reducing the segregation of Cu. The corrosion performance can be improved by increasing MG content and designing new MG with low Cu content.

#### 2.2.2 IGC mechanism

IGC is a locally selective corrosion occurring along a specific grain boundary displacement related to the chemical

and physical states of adjacent grains and the influence of environmental factors at grain boundaries [78]. IGC usually begins with the irregular arrangement of atoms at grain boundaries, which are usually corrosive regions in which atoms are loosely and disorderly arranged. Therefore, it has a large activity at the grain boundary. The influence of electrochemistry on the corrosion behavior of grain boundaries is mainly manifested by alloying elements in grain boundaries. Currently, the accepted mechanisms of IGC of SS are mainly divided into grain boundary dilution theory, intergranular  $\sigma$  phase precipitation theory, and grain boundary adsorption theory [79]. IGC and pitting are the main causes of failure of MMCs in Marine environment corrosion. IGC usually occurs because of the inhomogeneity of matrix and grain boundaries. There are alloying elements precipitation regions in grain boundaries of MMCs with alloy matrix. Owing to the potential difference between the precipitated area and the matrix, corrosion will occur at the grain boundary and form the IGC pathway. The precipitation of the second phase at the grain boundary is the main factor of IGC. The heating aging treatment of aluminum alloy can change the precipitate at grain boundaries from continuous to discontinuous, thus improving the corrosion performance [80]. These precipitates include grain boundary precipitates (GBPs), matrix precipitates, and precipitate free zone adjacent to GBPs.

It has been reported that grain size (i.e., grain boundary density) is an essential factor affecting the corrosion behavior of MMCs [81,82]. The addition of reinforcement can effectively refine the grain and has a positive effect on the corrosion performance. Ralston et al. [83] determined a similar Hal-Petch relationship between grain size (d) and corrosion rate  $(i_{corr})$  under different corrosion environments.

$$i_{\text{corr}} = a + bd^{-\frac{1}{2}},$$
 (2)

where a is the material constant and b is the environmentrelated constant. In a passive environment (b is negative), the corrosion rate of the aluminum alloy decreases with grain refinement, and a dense protective oxide film is formed on the surface. Therefore, the composites have stronger corrosion resistance. Smaller intermetallic compounds help to improve pitting resistance by reducing microcurrents and forming a continuous passive film. Ralston et al. [84] speculated that the matrix oxide might bridge the small precipitated phase, while the large precipitated phase could not be bridged, which would destroy the stability of the passivation film. Compared with 7050 alloys, TiC addition can refine the grain of aluminum alloy and the aging precipitates in the composite. The decrease in nucleation and growth driving forces caused by the large

consumption of interface holes and solute atoms should cause precipitate refinement. However, adding TiC particles can induce IGC and thus reduce the corrosion performance of the composites. The effect of TiC particles on the initiation and propagation of IGC in composites is mainly realized through the influence of the precipitate phase. TiC particles are mainly distributed along GBs. Preferential dissolution of interfacial sediments provides a continuous IGC channel and accelerates the IGC rate of GBPs. The corrosion propagation path is interrupted due to TiC particles in the composite, although the interfacial sediment is also dissolved in the corrosive environment. Therefore, these TiC particles have localized corrosion pits around them and do not affect IGC. The continuous distribution of TiC particles determines the initiation and propagation path of corrosion cracks. The relatively dispersed TiC particles (perpendicular to the ED) had the best corrosion resistance due to the corrosion channel disruption, whereas the particle chains parallel to the ED and with the best continuity were shown to have the most severe IGC.

#### 2.2.3 Stress corrosion mechanism

Stress corrosion cracking (SCC) is the degradation of the mechanical performance of materials because of physical stress and corrosive environments. SCC is a degradation or cracking process in corrosion-prone alloys (such as aluminum and steel). It occurs when three conditions exist simultaneously. Namely, the elements of the material alloy must be corrosion-prone, the tensile stress should be above a certain threshold, and a specific environment promotes cracking. Such failures occur with potentially susceptible metals and under conditions of use and often fail without any warning and lead to catastrophic failure. There are three mechanisms of SCC in Al alloy: 1) Anodic dissolution, preferential corrosion along grain boundaries, resulting in cracking. 2) Hydrogen-induced cracking - corrosion cracks are caused by local corrosion or concentrated stress; atomic hydrogen adsorbed on crack tip weakens grain boundary and leads to crack formation and propagation. 3) Rupture and cracking of passive film along grain boundaries [85]. Winkler and Flower [7] found in the study of 7XXX aluminum matrix composite SCC that the composite has a longer life under the same SCC condition. Compared with the metal matrix, the Ti-rich and Fe-rich phases have more negative polarity, which can generate local galvanic cells between the bulk aluminum and the fiber/matrix interface, leading to pitting corrosion. In addition, it is observed that cracks in the non-corrosive products along the GBs of the

metal matrix originate from the bottom of the resulting pits. SCC of MMCs is initiated by pitting or dissolution mechanisms, followed by hydrogen embrittlement crack propagation resulting from hydrolysis and acidification of the solution in the pit. Holroyd et al. [86] suggested that Mg can promote hydrogen embittering in aluminum by promoting hydrogen entry and formation of magnesium hydride at GBs, where SCC cracks could be nucleated. This theory also applies to the boundary between the reinforcement material and the metal matrix in aluminum composites. GBPs mainly control SCC sensitivity because the potential difference between GBPs and surrounding areas is greatest [87]. Coarsened GBPs have two advantages for SCC: 1) Reduce the preferential corrosion interface between GBPs and their adjacent areas. 2) Reduce the potential difference between GBPs and their adjacent periphery.

## 3 Analysis of anti-corrosion properties of Gr–metal composites

Gr has high thermal and chemical stability and excellent resistance to permeation and can effectively block the passage of gaseous atoms such as oxygen and water. Thus, it has excellent potential for application as a metal protective material [88,89]. Gr has made remarkable research progress in the field of metal corrosion protection as scientists have successfully achieved the preparation of large-area Gr.

### 3.1 Preparation mechanism of Gr-metal corrosion resistant composites

Pure graphene coatings, namely surface Gr systems, are deeply dependent on the interfacial structure to exploit the corrosion resistance of Gr [90] fully. Pure Gr coatings are typically made by assembling molecular building blocks into single/multi-layer Gr using "bottom-up" methods such as organic synthesis, thermal deposition, or chemical vapor deposition (CVD) [91,92]. The corrosion performance of copper in chlorine-containing environments can be significantly improved by only one or two layers of Gr [93]. Pingale [94] prepared Cu–Ni/Gr composite coatings by embedding graphene nanosheets (GNS) into a Cu–Ni matrix by electric co-deposition, as shown in Figure 5(a). Copper and nickel ions are adsorbed on the GNS surface, and GNS surrounded by Cu and Ni ions diffuse toward the cathode through the

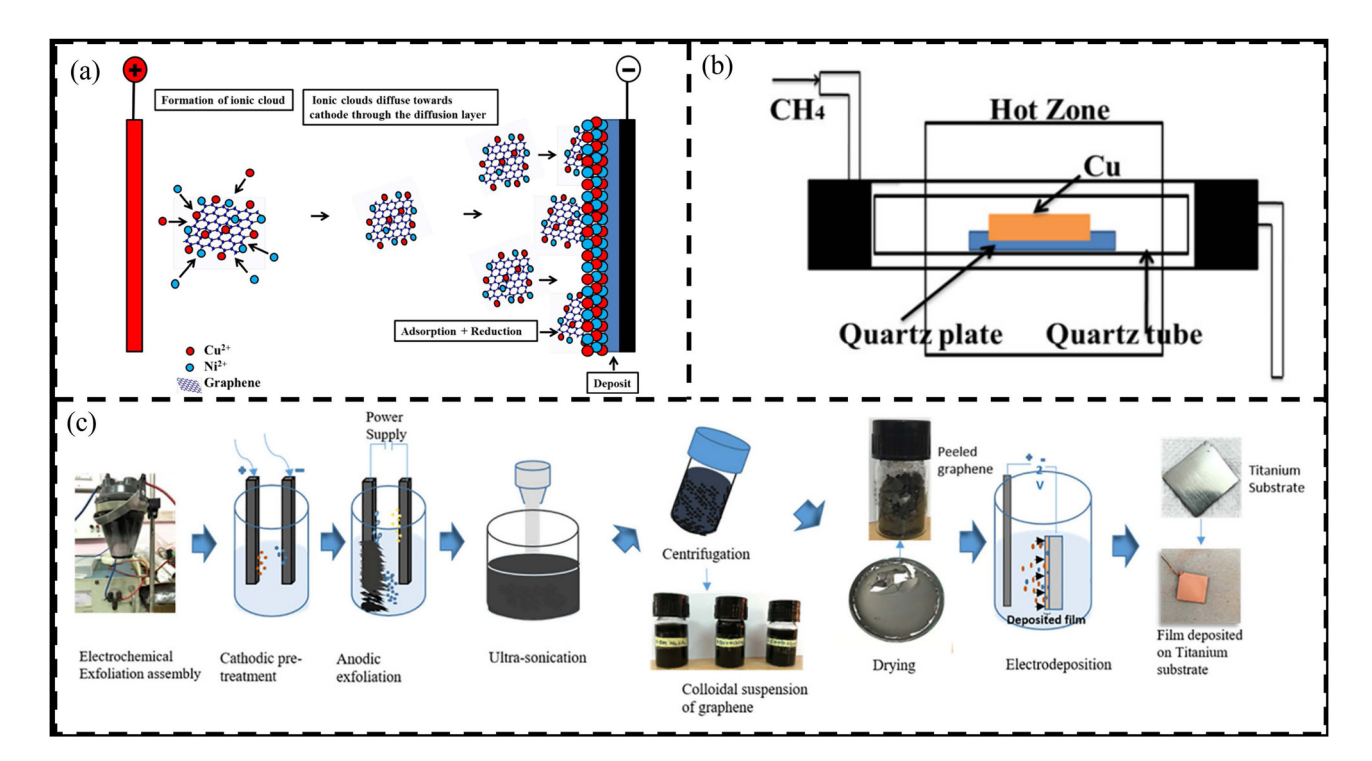


**Figure 5:** (a) Preparation of Gr–metal composites by CVD; (b) Schematic illustration of the home-built CVD equipment for graphene growth; (c) Schematic representation of electrochemical exfoliation of graphene, copper-graphene composite synthesis and flowchart of characterization techniques involved [77,78,85].

diffusion layer. Weak adsorption of GNS occurs on the cathode surface, and Cu and Ni ions are encapsulated and integrated into the Cu–Ni matrix at the cathode and GNS. Figure 5(b) shows a schematic of the CVD apparatus used for Gr growth. The system consists of a quartz tube furnace connected to a mechanical pump and a gas manifold. Gr is grown mainly by introducing a mixed gas stream containing H<sub>2</sub> and CH<sub>4</sub>. Gr was exfoliated from graphite rods, and then Gr-reinforced Cu matrix composites were prepared by electrodeposition, as shown in Figure 5(c).

Behera *et al.* [95] used mode atomic force microscopy (AFM) and observed the morphology of Cu and Cu–Gr composite films prepared on Ti substrates by electrodeposition. The three-dimensional AFM images of the synthesized coatings over the scanned region are shown in Figure 6(a–d). The figure shows continuous films, but the films are aggregated in a localized manner. The degree of agglomeration may affect the roughness of the film. The pure copper coating surface is less rough than other coatings. However, the agglomerate size is smaller

with the addition of more Gr particles. This result may be because the addition of Gr inhibits the grain growth during the deposition process.

However, the application of CVD is limited by the high cost of precursor gases, sophisticated equipment, the high processing temperatures required, and the wear resistance of ultrathin films [96,97]. Therefore, the preparation of Gr/polymer nanocomposite coatings has been proposed. For example, Gr/resin polymer composites were prepared directly by in situ polymerization by mixing Gr with resin monomers [98]. Gr is more flexible in composite coatings, and the content is usually in the range of 0.05-1.0%, which can significantly reduce the total cost of enhanced organic coatings [99]. Huh et al. [100] synthesized Gr/Cu composites were easily synthesized by growing monolayer graphene uniformly on the Cu surface by dropping acetone through the RTA method. Not only the corrosion properties of Cu will be significantly enhanced, but also the corrosion resistance of various metals and alloys will have potential offshore applications.

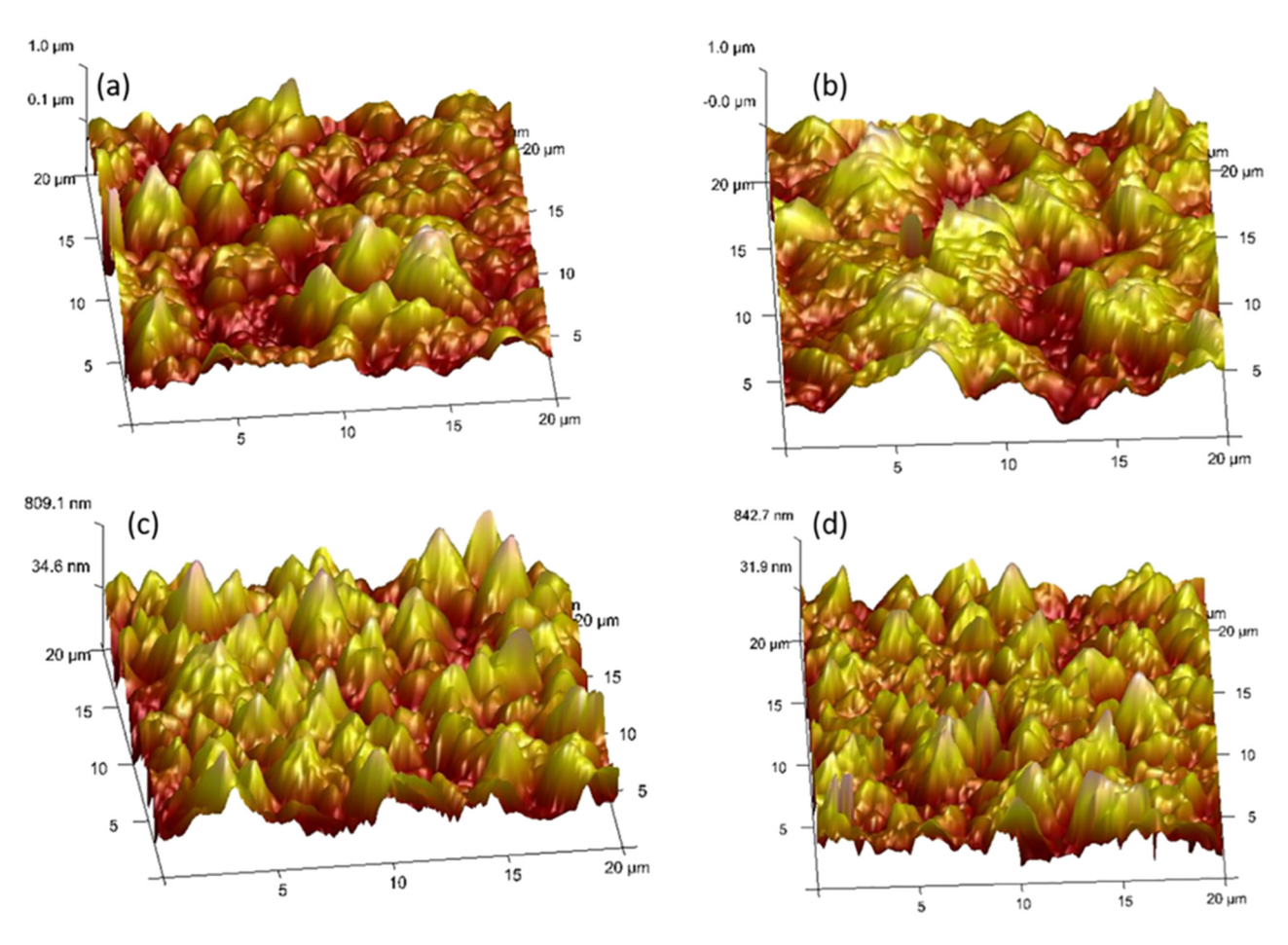


Figure 6: AFM surface topography of copper film and Cu-Gr composite films: (a) 0Gr; (b) 0.1Gr; (c) 0.3Gr; (d) 0.5Gr [95].

### 3.2 Optimization of anti-corrosion properties of Gr-metal composites

Incorporation of GNS into a metal matrix can improve strength, corrosion resistance, and hardness because of the structure and properties of Gr. The application of Gr coatings as a long-term corrosion protection technology on metal surfaces (mainly Cu, Ni, or Fe) is very promising in the near future [101]. Figure 7(a) shows the polarization curves of Cu-Ni/Gr composite plating fabricated by GNS with different concentrations in the plating solution [77]. As the concentration of GNS in the plating solution increased,  $E_{\rm corr}$  of the coatings increased from -0.382 to -0.224 V. The  $i_{corr}$  was significantly lower than the pure Cu-Ni coatings, indicating a better corrosion resistance of the composites. Zhu et al. [102] grew different thicknesses of Gr layers on the Cu substrate surface. Figure 7(b) shows that the  $i_{\rm corr}$  of the Gr-coated Cu samples were all reduced than those of the bare Cu substrate. The corrosion potentials ( $E_{corr}$ ) are shifted towards positive potentials of 15, 20, 50, and 70 mV, implying that the Gr layer protects the underlying metal substrate.

Apart from electrochemical experiments, salt spray tests are also important methods to evaluate the corrosion performance of materials. The corrosion resistance of Gr–metal composites is related to factors such as the thickness and defects of the Gr layer. Wu *et al.* [103] put Cu and Gr-coated Cu in a 48 h salt spray and tested the corrosion morphology. The results showed that the corrosion of the Gr-coated Cu substrate was lower than that of the treated Cu substrate. In addition, Zhu [102] concluded that the corrosion rate decreases with the thickening of Gr layers

through a 12 h salt spray test, which confirms the superior corrosion resistance of multilayer Gr. A Cu substrate covered by a single layer of Gr with corrosion spreading throughout the substrate and surrounding intact Gr islands, indicating that the corrosion started at the grain boundaries of the *in situ* grown Gr. With the stacking of the grown Gr layers, the corrosion of the wrapped copper is retarded. This is because the grain boundaries of different Gr layers are located differently. The upper Gr layer may cover the grain boundaries of the lower Gr layer and the diffusion of the corrosion product Gr grain boundaries is significantly inhibited.

## 3.3 Optimization of anti-corrosion properties of Gr-derived metal composites

In addition to Gr, polycrystalline graphene, graphene oxide (GO), reduced GO (rGO), and graphene quantum dots (GQDs) have become common Gr-based materials [104,105]. GO, with a relatively low cost, is considered promising for corrosion protection [105]. The oxygen-containing functional groups are highly processable and thus can be used as active sites for further modification or functionalization [106]. In addition to their intrinsic properties, these modifications can lead to versatility in surface chemistry and significantly alter and improve the properties of Gr.

He *et al.* [107] prepared silver-modified rGO reinforced Cu-based composites *via* hot-press sintering and tested the polarization curves, as shown in Figure 8. The polarization

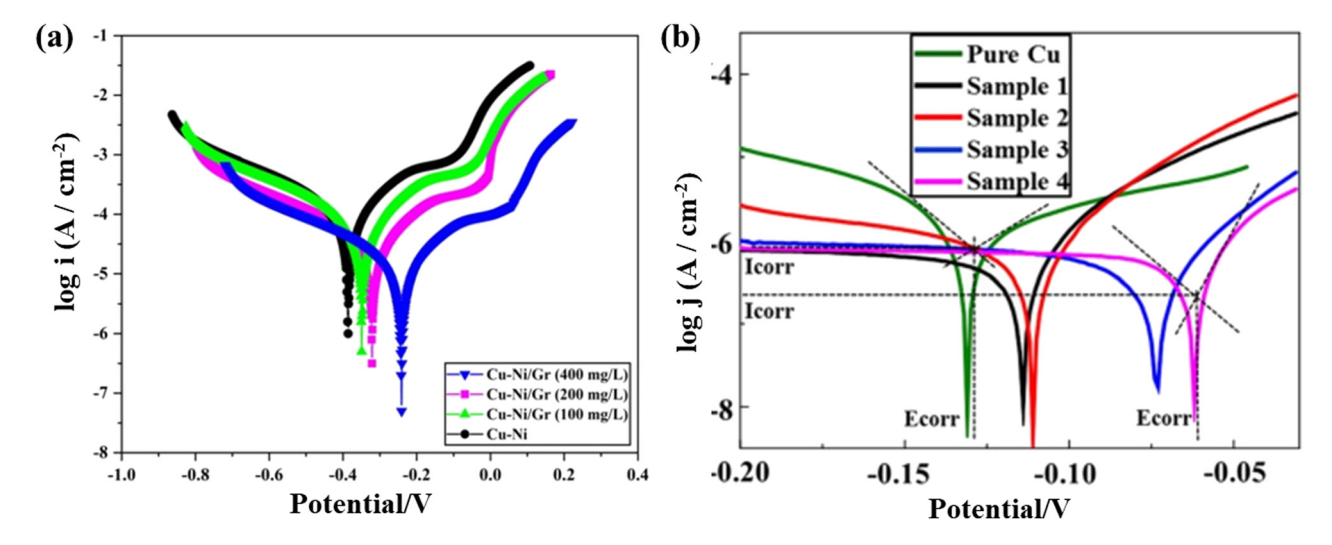


**Figure 7:** Electrochemical experimental results. (a) Polarization curves of Cu–Ni/Gr nanocomposite plating prepared with different concentrations of GNS in the plating solution. (b) Tafel plots of copper substrates coated and uncoated with different masses of Gr layers [102].

curves of the composites show a significant positive shift in corrosion potential compared to pure copper, indicating that the corrosion performance of the composites is much better than pure copper. The samples with silver-modified rGO content of 1.6 vol% had the highest corrosion potential, passivation interval, and best corrosion performance. Moreover, the  $i_{\rm corr}$  of the composite is much smaller, indicating that the coating forms a very strong protection. This improves the corrosion properties of copper even under very harsh conditions. From the overall results of the Tafel diagram, the rGO uniformly distributed in the Cu matrix acts as a strong passivation layer for ion diffusion and corrosion.

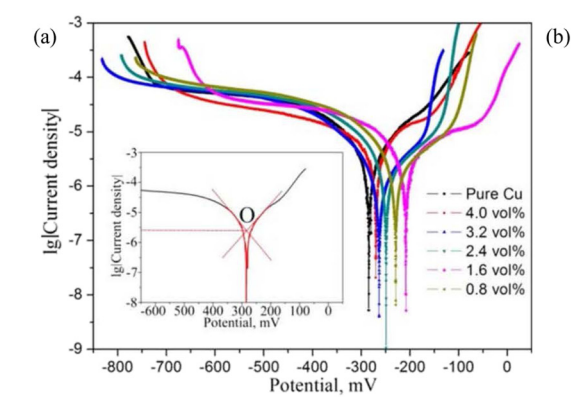
Many Gr films, Gr, and its functionalized composite coatings, and other Gr-like substances, such as GQDs and two-dimensional nanomaterials of GO, have been utilized as building blocks for corrosion protection, as shown in Table 2. This research on Gr-modified organic anticorrosive coatings can be divided into four aspects. First, the ultrathin 2D structure of Gr forms a shielding and barrier effect against corrosive media, retarding the penetration and diffusion of the coating [108]. The effect of shielding against corrosive solution requires a uniform dispersion of Gr and an orientation of Gr parallel to the metal surface. Furthermore, the anticorrosive properties of the coating are related to the shielding properties and depend on the bonding strength [109]. Therefore, enhancing the adhesion of coatings by bonding Gr-modified groups to metal surfaces is also the focus of research. Third, functional groups were modified on the active sites of GO to promote the formation of protective films, thus achieving self-healing defects and damages [110]. Eventually, the superior electrical conductivity of Gr was utilized to improve the cathodic protection effect of zinc-rich coatings on metals.

Common MMC coatings and MMC properties are shown in Tables 3 and 4.

# 4 Analysis of the corrosion protection mechanism of Gr composites in metallic materials

#### 4.1 Small size effect of Gr

The small size of Gr can fill the pores and defects in the coating, which prevents and retards the infiltration of small molecule corrosive media into the metal substrate to a certain extent. It also enhances the physical isolation and the anticorrosive properties of the coating. Wang et al. [16] cold sprayed Al/Gr coatings using Gr-coated Al powder having lower porosity than non-Gr-modified coatings. As the Gr content increases, it affects the formation of metallic bonds between metals in contact with each other. The agglomeration of Gr will also decrease the densities. Therefore, appropriate content and homogeneous dispersion of Gr can give full play to its small size effect. To improve the Gr dispersion, Cui et al. [131] used polydopamine (PDA) to modify Gr and fabricated a PDA-modified Gr/epoxy resin composite coating. The well-dispersed PDA-modified GNS filled the pores of the epoxy resin. It makes the coating denser, inhibits corrosive media penetration, and improves epoxy resin adhesion. Meanwhile, the modification of Gr by PDA makes the Gr less prone to curling, has a more effective aspect ratio, and extends the diffusion path of electrolytes. Um et al. [155] investigated the



Composites	$E_{corr/}(mV)$	$I_{corr/}(\mu A cm^{-2})$
Pure Cu	-285.2	2.38
0.8 vol%	-229.3	1.25
1.6 vol%	-207.8	0.74
2.4 vol%	-249.2	1.48
3.2 vol%	-263.3	1.61
4.0 vol%	-270.1	1.72

Figure 8: (a) Tafel polarization curves of pure Cu and composites. (b) Electrochemical corrosion parameters of pure Cu and composites [107].

 Table 2: Common coating material properties

Materials	Coating structure	Substrates	Characterization	Coating properties	Ref.
Gr films	CVD growth of Gr films	Cu	Electrochemical test in NaCl solution	The impedance of the Cu substrate was significantly increased, and the corrosion currents of both anode and cathode were reduced by 1–2 orders of magnitude, demonstrating the superb corrosion resistance of Gr films	[63]
Gr	Gr/epoxy nanocomposite coating	I	Local electrochemistry and scanning vibrating electrode technology	Compared to pure epoxy coatings, coatings with Gr content of 0.1% (volume fraction) showed better corrosion resistance	[111]
	Epoxy primer and polyurethane topcoat, curing agent and thinner are mixed with different proportions of Gr after the coating is finished	7075-T6 aluminum alloy sheet	Polarization curve and AC impedance of coatings	When the Gr addition is 0.2%, its self-corrosion current density is the smallest. Its impedance modulus and capacitive arc radius are the largest, and the corrosion resistance is the best	[112]
Hexagonal boron nitride (h-BN)	h-BN reinforced polyimide (PI) coating	SS	Water vapor impermeability test	The water vapor transport rate of PI/5 wt% h-BN composite coating was reduced by 84% compared to that of pure PI	[113]
	CVD growth of monolayer h-BN films	Cu	Density functional theory (DFT) calculation and experimental tools	The impermeability of h-BN to O <sub>2</sub> is comparable to that of graphene, and tests conducted after 160 days of aging in ambient environments confirm the long-term corrosion resistance of h-BN	[114]
	Monolayer CVD-grown h-BN films Boron nitride quantum dot modified h-BN reinforced waterborne epoxy resin (WEP) coating	Cu Carbon steel	Electrochemical test in sodium hydroxide solution Electrochemical tests in 3.5 wt% NaCl solution	CVD-grown h-BN films reduce the corrosion rate by an order of magnitude compared to pure copper WEP/0.5 wt% BNQDs h-BN composite coating reduces corrosion rate by an order of magnitude compared to	[115]
05	Alternate coating of GO/epoxy self-assembled coatings prepared by spin coating method	I	Kinetic potential polarization test in 3.5% NaCl solution	pure WEP  Steel specimens protected by 5 layers of GO-6 epoxy coatings with 17 µm thickness corrode 20 times slower than auro apparented executions.	[117]
Resorbed GO	Uniform crack-free rGO-PVPBM composite coating obtained by CVD deposition on copper foil	σ	Corrosion resistance test in 3.5% mass fraction NaCl solution	Compared to PVPBM coating, rGO-PVPBM composite coating has 3.7 times higher crack expansion resistance	[118]
GQDs	Silane-functionalized GQDs (f-GQDs) reinforced epoxy composite coatings	Low carbon steel	Electrochemical tests in 3.5 wt% NaCl solution	Epoxy resin/0.5 wt% f-GQDs composite coating reduces corrosion rate by an order of magnitude compared to pure epoxy resin	[119]

Table 3: Common MMCs coating properties

Materials	Coating structure	Substrates	Characterization	Coating properties	Ref.
Gr	Gr/Ni composite coating	Mild steel	Electrochemical test in 3.5 wt% NaCl solution	The surface morphology of Gr in Ni coating changes to fine grain coating, the grain size decreases, and the hardness increases. The corrosion resistance of the composite coating is better than that of the pure Ni coating	[120]
Gr	Gr/Ni composite coating	n O	Electrochemical test in 0.5 M NaCl solution	times slower than dditives, and the er than that of the	[121]
Ğ	Novel functional gradient Gr/Ni composite coating	Mild steel	Electrochemical workstation was used to measure the electrochemical behavior of the coating in ${\sf CO}_2$ saturated seawater	itent and grain size increase with the gradient of ickness. The corrosion current densities of FG Nisare one and three orders of magnitude smaller of uniform Ni-Gr composite coatings and mild nas, respectively	[122]
Ğ	Sandwich Gr/Ni composite coating	AZ91D magnesium alloy	Electrochemical test in 3.5 wt% NaCl solution	Gompared with single Gr/Ni composite coatings, sandwich Gr/Ni composite coatings have better long-term corrosion resistance. It comes from the multi-interface passivation film mechanism brought by the multi-layer design, which greatly delays the time of corrosive media invading the substrate	[123]
09	GO/Al <sub>2</sub> O <sub>3</sub> /Al composite coating	AZ91D magnesium alloy	Electrochemical test in 3.5 wt% NaCl solution	The mechanical properties of the composite coatings were significantly improved by the addition of GO (about 600%). Due to its high surface area, GO acts as a bridge between alumina nanoparticles. The corrosion resistance is almost twice that of the matrix alloy. This is attributed to GO's role in preventing crack formation in the coating microstructure.	[124]
Gr	AI/(Al <sub>2</sub> O <sub>3</sub> -G) composite coating	n O	The cyclic polarization curve and impedance behavior of the coating were tested in 3.5 wt% NaCl static solution	The cold-sprayed Al/Gr coating has good corrosion resistance and strong repassivation ability, because Gr transforms its longitudinal accelerated pitting corrosion mechanism into tangential surface corrosion	[16]
Gr	Gr/NiP	O.	Electrochemical test in 3.5 wt% NaCl solution	The Cu-Gr-NiP coating showed good resistance to electrochemical degradation. The enhanced corrosion is attributed to the uniform dispersion and grain refinement of Gr	[14]
Gr	Cu-Ni/Gr nanocomposite coatings were prepared by electrocodeposition	Carbon steel	Electrochemical tests in 3.5 wt% NaCl solution	The addition of GNS stabilized the corrosion potential and improved the corrosion resistance	[94]
09	Electrodeposition of Zn–GO composite coating	Low carbon steel	Electrochemical tests in 3.5 wt% NaCl solution	The permeability resistance of GO hinders the penetration of electroactive media and reduces the oxidation degree of zinc layer, thus slowing the corrosion rate	[125]

Table 4: Common MMC properties

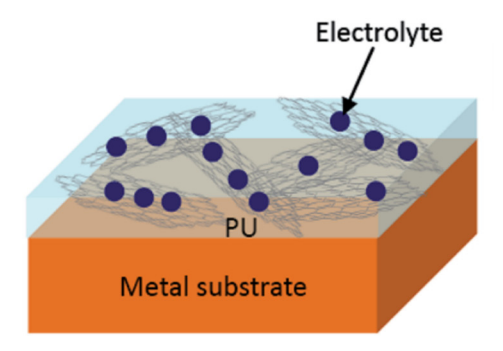
Materials	Structure	Characterization	Properties	Ref.
Gr/graphite	AI/Gr and Al/graphite composites	Electrochemical test in 3% NaCl solution	The corrosion resistance of Al in NaCl solution is 3 (corrosion resistance), and the corrosion resistance of aluminum composites is 4 (fairly corrosion resistance). At the same carbon content, the corrosion rate of Al-graphite composites is about three times that of Al-graphite composites	[126]
Gr	Gr/Mg composite	Electrochemical test in different salt electrolytes (NaCl, KCl, and Na- $50_a$ )	nical tests showed that the corrosion rate decreased sharply ferent aqueous solutions, NaCl, KCl, and Na $^{5}$ Co $^{4}$	[127]
Gr	Gr (0.1, 0.25, and 0.5 wt %)/Mg composite	Electrochemical test in 3.5% NaCl solution	Due to Gr agglomeration, the corrosion performance of the composites decreases. The microelectric reaction occurs because magnesium behaves as an anode while graphene behaves as a cathode	[128]
Functionalized few layered graphene nano-sheets (FLGNs)	FLGNs/Cu composites	Electrochemical test in borate buffer and 3.5 wt% NaCl solution	The corrosion resistance of the composites in borate buffer and NaCl solution was improved	[62]
Ğr.	Gr/Cu	Electrochemical test in 3.5% NaCl solution	The addition of or reduces the potential difference between the two poles of the corrosion unit, slows down the corrosion rate, reduces the diffusion rate of copper ions in the oxide film, increases the resistance of the composite material, and improves the corrosion resistance of Gr/Cu composite material	[129]
Gr	Dispersed Gr-reinforced Al composites	Electrochemical test in 3.5% NaCl solution. IGC test and first principles calculations	The addition of GNPs as long-term corrosion inhibitors in Al matrix composites can simultaneously enhance the energy barrier of vacancy formation, Cl entry, and charge transfer.	[17]
Gr	Gr/Cu laminated composites	Electrochemical test in 3.5% NaCl solution	Gr is arranged in parallel to isolate solutions and ions. The layered structure changes the corrosion path	[154]
Gr	Gr/2024Al composite	Electrochemical tests in 3.5 wt% NaCl solution	.024Al composite samples at 560°C t MPY, respectively	[130]

effect of Gr size on the anticorrosion performance of polyurea (PU) composite-coated Cu substrates using electrochemical techniques. The EIS results indicated that the Gr-incorporated PU composites with Gr sizes less than 2  $\mu m$  provided better corrosion protection for the Cu substrate. This is because the small-sized GNS could be uniformly dispersed in PU, thus generating an extended diffusion pathway to inhibit the penetration of the corrosive medium.

#### 4.2 Gr flake structure role

Gr is an extremely thin sheet structure that can be layered to form a dense physical barrier in the coating. Small molecules of corrosive media can hardly pass through this dense insulation layer, so the anti-corrosion coating mixed with Gr has a solid physical insulation effect. The premise of the shielding property of Gr/GO materials is that their planes are distributed in a direction parallel to the substrate. This is because the intrusion of corrosive media is spread from the coating surface to the substrate. Only a shielding effect parallel to the direction of the substrate can effectively block the intrusion of corrosive agents. Gr/GO-modified materials with vertical or haphazardly oriented distribution cannot meet the structural denseness of the coating and are contrary to the shielding concept [132]. Figure 9 demonstrates the mechanism of action of the titanate-modified graphene oxide (TGO) electrolyte in PU coating with three-dimensional random distribution and parallel arrangement. It shows a zigzag penetration path when the TGO in the composite coating is randomly distributed in three dimensions. And when the TGO layer is self-aligned parallel to the substrate surface, a layer protection network is formed, which gives full play to the surface barrier effect of the modified GO and blocks the electrolyte from penetrating the coating [133]. It is obvious that the ordered arrangement of GO composites can solve the problem of defects in coatings and improve the corrosion properties of coatings. However, the ordered arrangement of Gr/GO composites in coating applications needs more systematic studies. Moreover, the currently used methods have certain limitations, and achieving the ordered arrangement in practical applications is more difficult.

To further enhance the shielding property of the coating, the ordered arrangement of Gr can be achieved by improving the dispersion. There are mainly ordered alignment methods such as applied electric field induction, magnetic field induction, and layer-by-layer selfassembly [134]. Magnetic field-induced ordered alignment is mainly solved by preparing magnetic Gr materials or loading magnetic substances (Fe<sub>2</sub>O<sub>3</sub> or Fe<sub>3</sub>O<sub>4</sub>) onto the surface of the Gr. However, this method requires the presence of a uniform horizontal magnetic field and is costly to operate. Pang et al. [135] investigated the orientation of GNS in polystyrene coatings under the effect of electric field induction. The results show that under an electric field, the conductive particles can cross the polymer's hindrance and adjust the curling degree. The distribution tends to be parallel to the direction of the electric field, forming multiple conductive channels. The orientation in the electric field-induced ordered arrangement is mainly due to the dipole moment of water molecules in the first hydrated layer on the Gr surface that appears to respond to the orientation under the electric field, tending to be parallel to the direction of the Gr plane and the electric field. Zhao et al. [136] successfully prepared ultrathin multilayer anticorrosion coatings (PVA/GO) of polyvinyl alcohol (PVA) and GO using exfoliated GO as substrates by a bottomup layer-layer assembly method. The ordered arrangement of organic and inorganic layers was found to result in significantly improved mechanical properties, which was attributed to the well-layered structure of GO in the polymer matrix, as well as the high degree of planar orientation and nanoscale pore filling.



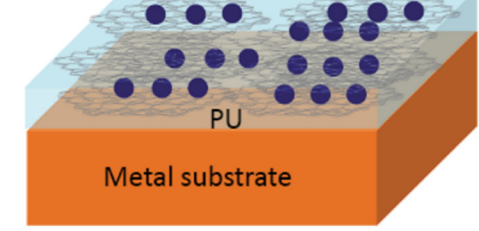


Figure 9: Schematic diagram of TGO/PU coating [133].

The Gr layer number also affects the corrosion performance. The corrosion resistance of the composites was found to increase and then decrease with the increase in the number of Gr layers [103]. The metal substrate under the Gr boundary is directly exposed to a severely corrosive environment for monolayer Gr, as shown in Figure 10(a). Corrosive media can easily penetrate the defects of Gr and cause severe corrosion to the metal. The anti-corrosion effect of bilayer Gr is effective, as shown in Figure 10(b). In the overlapping structure of bilayer Gr, it is difficult for chloride ions to reach another defect in the lower Gr layer by lateral diffusion, and the path of chloride ions to get the interface between Gr and metal matrix is prolonged. For multilayer Gr coatings (Figure 10(c)), defects in adjacent Gr layers are joined together, creating a lot of corrosion paths from the top Gr layer to the interface between the Gr and the metal substrate. In addition, Cl<sup>-</sup> is difficult to transfer between the two Gr layers by lateral diffusion. The highdensity defect leads to a shortened corrosion pathway and easier penetration of the corrosive medium into the Gr coating. When Cl<sup>-</sup> reaches the Gr/metal interface, galvanic coupling corrosion begins, further accelerating the corrosion of the metal substrate.

#### 4.3 Impermeability of Gr

The high impermeability of Gr can be attributed to two factors: the narrow six-membered ring of carbon in GNPs and the dense delocalized cloud of  $\pi$ -orbitals of Gr that can repel any atom or molecule at room temperature. Sun *et al.* [156] used graphite or h-BN monocrystals to prepare a

novel micrometer-sized well encapsulated by Gr, as shown in Figure 11(a). The result showed that the Gr membrane was impermeable to several gases, including He, N2, O2, Ne, Ar, Kr, and Xe. Jiang et al. [157] investigated the selectivity and permeability of Gr with designed sub-nanometer-sized pores using DFT calculations (Figure 11b). Gr with a hydrogenpassivated pore (2.5 Å × 3.8 Å) exhibited a high barrier for  $CH_4$  (1.6 eV), whereas it was easy to permeate  $H_2$  (0.22 eV), affording an extremely high selectivity for CH<sub>4</sub>/H<sub>2</sub>. As a result, perfect Gr sheets are impermeable to most species, but the defects and openings in Gr provide diffusion channels for these species. It is generally believed that the impermeability of Gr is highly related to its quality, temperature, molecular properties, and other external factors. Theoretical results indicate that the barrier energy decreases exponentially with an increase in the defect size of Gr [158]. The energy barrier of different atoms and molecules is shown in Table 5. Perfect Gr sheets are impermeable to most species, but the defects and openings in Gr provide diffusion channels for these species.

The contact angle between water and Gr is very large. The wettability to water is very weak, and water molecules are hardly absorbed by Gr. The Gr will block the water molecules outside the coating in the epoxy resin. Then, the water molecules cannot contact the metal substrate surface, thus reducing the corrosion. In addition to incorporating Gr as a nano-filler into coatings to enhance corrosion protection, some researchers have also prepared multilayer Gr-based anti-corrosion coatings directly on the surface of metal substrates. Xu *et al.* [137] prepared multilayer Gr anti-corrosion coatings with a thickness of 14 nm by introducing Ti layers onto the mild steel surface by vacuum deposition and then immobilizing Gr on its

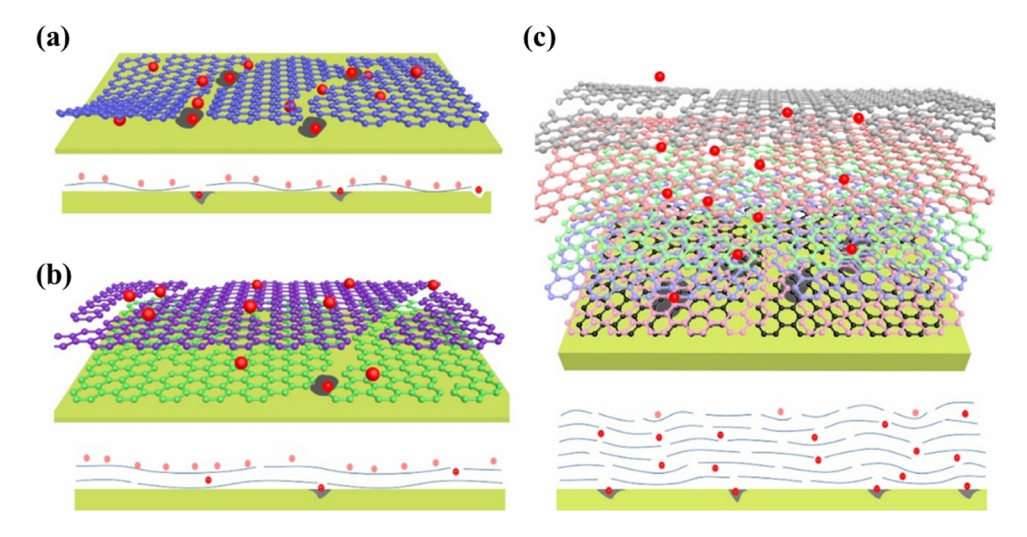


**Figure 10:** Schematic diagram of corrosion protection mechanism of Gr coating with different number of layers: (a) Single layer; (b) Double layers; (c) Multi layers [103].

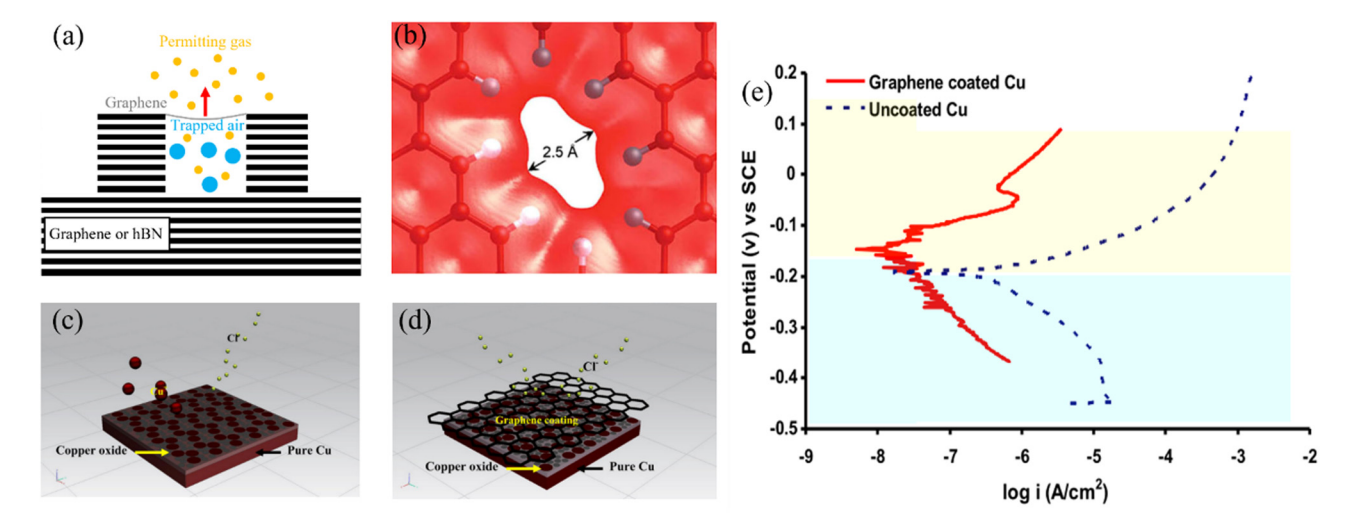


**Figure 11:** (a) Schematic of monocrystalline containers sealed with Gr [156]; (b) electron-density isosurface of a hydrogen-passivated pore in Gr [157]; (c and d) schematic of the corrosion mechanism occurring on uncoated Cu (top) and Gr coated Cu (bottom) specimens; (e) potentiodynamic polarization of the Gr coated and uncoated Cu [93].

surface by mechanical ball milling method through Ti-C bonding. The results showed that the corrosion rate of mild steel decreased from 794.5 to 8.2 nm/day after being covered by a multilayer Gr coating, which is nearly 2 orders of magnitude lower than that of bare steel. It indicates that the Gr coating acts as an impenetrable barrier on the surface of mild steel, significantly reducing its corrosion rate. To further improve the anti-corrosion effect, it is more common to modify Gr hydrophobically before laminating it with the coating, or to laminate it with the

Table 5: Energy barrier of different atoms and molecules

Atom/ molecule	Gr	Energy barrier (eV)	Ref.
CH <sub>4</sub>	All-hydrogen passivated porous Gr	1.6	[157]
H <sub>2</sub>		0.22	[157]
Oxygen atom	Pristine Gr	16.34	[89]
02	Pristine Gr	10.12	[89]
Cu	Pristine Gr	30.62	[159]
Oxygen atom	The center of eight-ring defects	8.014	[160]
	The center of seven-ring defects	10.36	[160]
	The center of six-ring defects	21.81	[160]
	The center of five-ring defects	21.36	[160]
Li <sup>+</sup>	Pristine Gr	7.92	[161]
	Gr with single vacancy	3.6	[161]
	Gr with double vacancy	1.31	[161]
	Gr with Stone–Thrower–Wales defects	2.98	[161]

coating first and then modify it hydrophobically. Uzoma *et al.* [138] used F–Si to modify GNS and then compounded them with hydrophobic siloxane-acrylic resins. On the one hand, the F–Si modification improves Gr dispersion in siloxane-acrylic resin. On the other hand, the good hydrophobicity of the composite coating makes it difficult for corrosive media to wet it, thus enhancing the anticorrosion performance of the composite coating.

Raman [93] pointed out that during the kinetic potential polarization, as shown in Figure 11(e), the intercepts of the cathodic and anodic diagrams of the Gr-coated copper were significantly shifted in the positive direction. The anodic current density of the Gr-coated specimen is much lower than that of the uncoated specimen. This indicates that corrosion susceptibility is reduced, which in turn indicates that the Gr coating significantly reduces the dissolution of Cu. The corrosion properties of Gr-coated Cu were at least 1.5 orders of magnitude higher than that of uncoated Cu. The protective effect of the Gr layer is related to its water resistance. Cu oxides formed by Cu under environmental conditions do not protect it from Cl<sup>-</sup>, while the impermeable and inert Gr layer protects the Cu film from electrochemical degradation, as shown in Figure 11(c and d).

#### 4.4 Gr conductive effect

The unique structure of Gr gives Gr fast electrical conductivity. Electrons will pass through the Gr to the metal coating. The cathodic electrons do not occur directly on the metal but react directly with the coating. This slows

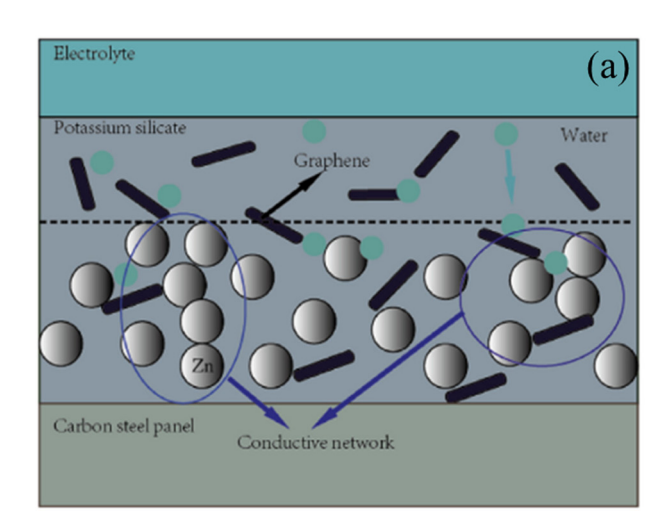
down the production of iron hydroxide and reduces the dissolution of the metal. It also protects the metal, which is done by using the electrical conductivity of Gr to protect the metal substrate. The closely stacked Gr forms highly efficient conductive channels. In the early stage of corrosion occurrence, it can transfer the electrons lost in the anodic reaction to the coating surface in time, effectively delaying the further occurrence of corrosion reaction. When applied in zinc-rich anti-corrosion coatings, it can form electron transfer channels with metallic zinc powder due to the high electrical conductivity of Gr/GO. There is no need for a large amount of zinc powder to accumulate closely, enhancing the effective zinc powder utilization rate, as shown in Figure 12 [139,140]. By introducing Gr into the zinc-rich primer, the conductive effect of Gr is fully utilized to replace part of the zinc powder. Moreover, it bridges with zinc powder to form a conductive pathway to enhance the cathodic protection effect of the coating [141].

### 5 Research progress of Gr composites

The method of Gr in metal protection is mainly realized through three methods: 1) Pure Gr film; 2) Gr composite coating; 3) Metal/Gr composites. Boehm [142] first demonstrated that Gr films could prevent Cu and Cu/Ni alloys from oxidizing by air. Pure Gr film could act as a barrier to the metal substrate to prevent metal corrosion. Wang *et al.* [143] compared the protective effects of single-layer Gr and double-layer Gr films and confirmed that

double-layer Gr has a better anti-corrosion effect than single-layer Gr. Corrosive media such as chloride ions easily penetrate the Gr defects, causing severe corrosion. In the overlapping structure of bilayer Gr, it is difficult for Cl<sup>-</sup> to reach another defect of the underlying Gr by lateral diffusion, and the path of chloride ions to reach the Gr/matrix interface is prolonged. Wu et al.'s [103] study showed that Gr's corrosion performance increased with the increase in the number of layers, and the corrosion performance decreased with the increase in the number of layers. For multilayer Gr coatings, defects in adjacent Gr layers are joined together, creating many corrosion paths from the top layer of Gr to the interface between Gr and the metal matrix. In addition, lateral diffusion makes chloride ions difficult to transfer in two Gr layers. The high-density defects lead to a shorter corrosion path, and the corrosive medium is easier to penetrate the Gr coating. When Clreaches the Gr/metal interface, galvanic corrosion starts, further accelerating the corrosion. Prasai et al. [144] grew multilayer Gr films on copper and nickel surface to study their corrosion properties. The corrosion rate of the copper film with pure Gr is seven times that of the copper film. Ni coated with multiple Gr films corroded 20 times more slowly, while Ni coated with 4 layers of mechanically transferred Gr corroded 4 times more slowly than a bare Ni.

However, the defects of Gr are permeated by  $O_2$  and solution, resulting in the corrosion of the matrix. Schriver *et al.* [145] found that the preservative effect of Gr only lasts for a short time (minutes to hours). Fewer defects inside Gr can solve these problems if we want to use Gr to achieve long-term anticorrosive effects. Wu *et al.* [103] studied the corrosion behavior of Gr coatings with different layers and



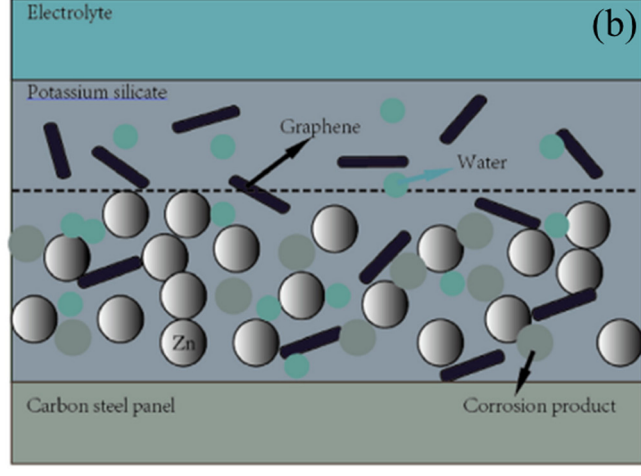


Figure 12: Sketch map of the coating in (a) cathodic protection stage and (b) barrier protection stage.

found that the corrosion performance of Gr mainly depends on the density of defects rather than the number of layers. Ren et al. [146] first used N-doped graphene (NG) as a passivation layer to protect the metal surface. NG has better corrosion resistance than pure Gr. The addition of N atoms and the topological defects on the Gr lattice reduces the electrical conductivity and inhibits the corrosion of copper.

The anti-corrosion mechanism of Gr composite coating has been described in Section 3. In 2012, Chang et al. [147] first proposed using Gr/polyaniline composite coating to prevent steel corrosion. Roding et al. [148] calculated the orientation, size, and amount of Gr. Under the geometric effect, about 0.2 w/w% Gr can reduce the diffusivity by 90%, and about 1 w/w% Gr can reduce the diffusivity by 99%. Due to the high surface area and van der Waals forces of Gr, the dispersion of Gr in the coating matrix is a problem that needs to be solved. Some researchers have used physical methods such as stirring, ball milling, and ultrasonic treatment to disperse Gr [149,150]. The physical dispersion method has a low cost, but the dispersion effect could be better, so it is usually used as an auxiliary method for dispersion. Currently, the covalent functionalization of Gr is the most widely used. Covalent functionalization can add active groups such as carboxyl, hydroxyl, and epoxy bonds to Gr through various chemical reactions. He et al. [151] used the covalent interaction between the carboxyl group of GO and the amide group of ethanolamine to disperse Gr in an aqueous solution with good stability. Compared with pure Gr, GO not only has better dispersion but the oxygen-containing functional groups of GO can also hinder the penetration of corrosive media [152]. Ramezanzadeh et al. [153] studied the interfacial interaction between the mixed epoxy coating containing functionalized GO and the steel matrix. They found that adding GO effectively improved the binding strength and durability of the epoxy coating and the steel surface. In addition, the non-covalent functionalization method for dispersing Gr has also been widely used. Wang et al. [16] achieved stable dispersion of 2D GNS in water-based resins through non-covalent  $\pi$ – $\pi$ interactions between Gr and poly(2-butylamine) (P2BA). The P2BA hybrid promotes the formation of passive oxides on the steel surface. It inhibits the penetration of aggressive anions such as chloride, water, and oxygen into the steel substrate through the coating. Wang et al. [16] proposed a method of coating Gr on Al particles for cold spraying and successfully prepared low-defect parallel Gr/Al composite coatings. Uniformly dispersed Gr can effectively improve the defects of the coating, and parallel Gr distribution can effectively hinder the longitudinal propagation of corrosion cracks. The arrangement direction of Gr also provides an effective idea for Gr protection in MMCs. Jin et al. [154]

designed and fabricated Gr-encapsulated Cu (Cu@Gr) micro/ nano sheets, which were then sintered to form layered Cu matrix composites to achieve parallel distribution of Gr. Dispersed Gr has a good anti-corrosion effect, and its performance depends on the orientation of the Gr. Anisotropy can be understood in terms of Gr orientation and corrosion paths due to blocking effects. The parallel distribution of Gr can effectively hinder the longitudinal propagation of corrosion media and cracks and fully exploit the structural characteristics of 2D Gr.

#### 6 Challenges and perspectives

The environmental factors in the marine environment are complex high temperature, humidity, salinity, and other environments, as well as the microorganisms in the ocean, which will accelerate the corrosion. To reduce corrosion, Gr can be compounded with coatings and metal materials to give full play to the small effect of Gr to reduce porosity. In the harsh environment of marine corrosion, Gr anticorrosion coatings can not only be used for the outer layer of marine equipment for heavy corrosion protection but can also be used for the interior of ships, such as super-fast heat dissipation in parts of high heat energy electromechanical equipment, large electronic components and large CPUs, high power radars, etc. Its effect is remarkable Gr's high thermal conductivity can help important parts dissipate heat and reduce temperature to improve corrosion properties. In recent years, research on graphene in metal corrosion protection has been reported one after another, and significant progress has been made. The graphenebased anti-corrosion coating can improve the strength and friction performance while providing good protection to the metal substrate, which is a new type of anti-corrosion coating with green, stable nature and excellent corrosion resistance. However, as a new carbon material, the application of graphene still faces many challenges.

More attention to the explicit description of the distribution of Gr and interface will help better understand the relationship between complex interfaces and corrosion performance. This relationship can pave the way for optimizing the internal coating structure. In addition, there needs to be more effective processing ways to achieve Gr's alignment and spatial organization in composite coatings. Second, the existing preparation process needs to be improved to obtain high-quality and large-area Gr. Moreover, this technology is still in its infancy. The corrosion resistance mechanism of Gr still needs further in-depth study to guide the development of new corrosion protection technologies.

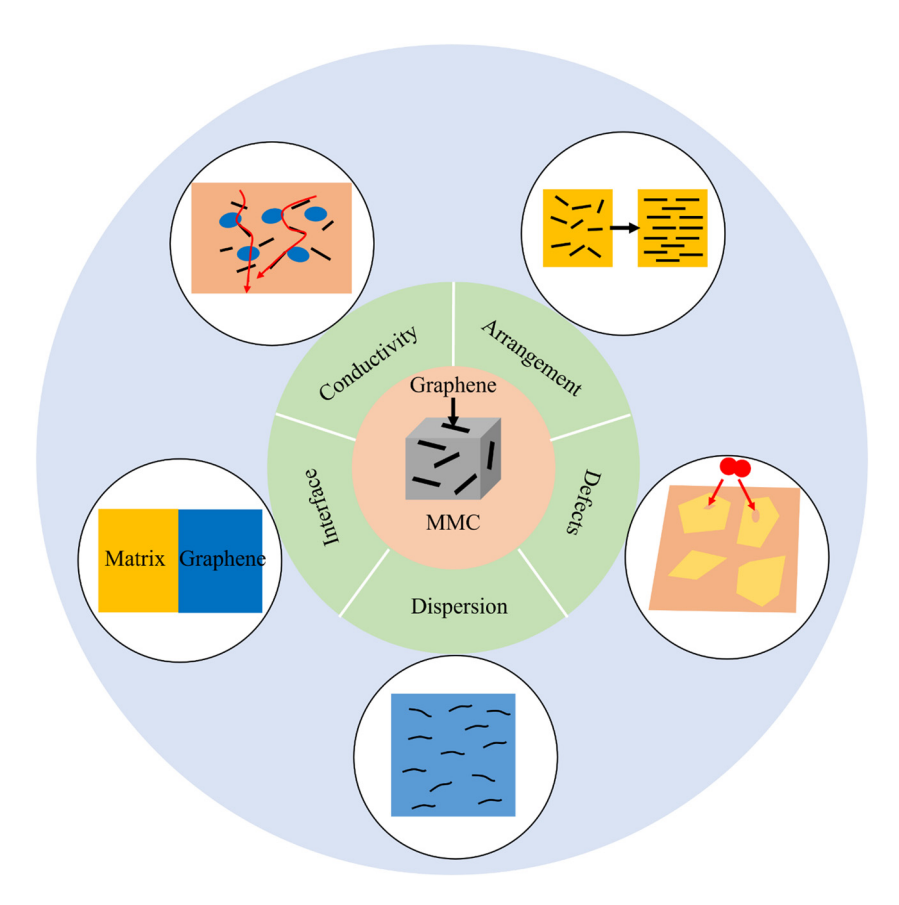


Figure 13: Schematic of the challenges for MMC reinforced with Gr.

With further research, Gr is expected to become an ideal metal anti-corrosion coating with its unique and outstanding performance.

Improving the properties of graphite-enhanced cathodic protection coatings and self-healing coatings is a difficult task. Specifically, by optimizing the component content (Gr/Zn content ratio) and the internal structure of the coating, both electron transfer and shielding protection can be promoted. Regarding self-healing coatings, attempts should be made to achieve multiplexed repair for repeated healing and improved healing efficiency. It is also a challenge to manufacture multifunctional coatings with intelligent synergistic properties such as anti-pollution, self-healing, anti-corrosion, and self-cleaning. Gr-based coatings need to be studied using advanced experimental studies and theoretical methods to gain insight into the protection mechanisms of Gr-based coatings. Attempts should be made to establish "quantitative links" and "multi-scale bridges" between findings at different levels. Multidisciplinary collaborative research studies must achieve a breakthrough.

When the metal surface coating fails, the material's corrosion resistance plays an important role. Based on a review of the development of MMC reinforced with Gr and

composite coatings, fabrication methods and barrier performance have demonstrated significant progress. However, there are still numerous roadblocks and challenges to be addressed and overcome using fundamental science and industrial technology, as illustrated in Figure 13. The defects in MMC reinforced with Gr are mainly the defects of Gr and composites. The defects of Gr weaken the barrier performance of Gr and cause a corrosion-promoting effect. Although studies have demonstrated that large-area continuous Gr can block the penetration of oxidizing and corrosive species to a certain extent in short-term experiments, oxidation and corrosion still occur at defective sites. For MMC reinforced with Gr, the dispersion, content, size, arrangement, interface, and conductivity of Gr in the composites are critical factors affecting their anticorrosion properties. In MMC reinforced with Gr, the metal/Gr interface is an essential factor affecting composites' mechanical properties and corrosion properties. Good interface bonding is beneficial for reducing defects and improving mechanical properties and corrosion properties. Electroless plating and surface modification were widely used to strengthen the metal/Gr interface. Covalent and noncovalent modification methods can improve Gr dispersion

in the matrix. However, toxic chemical agents may harm human health and the environment. The structure of Gr is prone to damage during surface modifications. Thus, developing an eco-friendly and non-destructive dispersion technique is required for further exploration. Theoretical and experimental results suggest that Gr aligned parallel to the corrosion surface provides an optimal barrier against corrosive media. Rolling, vacuum filtration, flake powder metallurgy, freezing casting, electrophoresis, preform molding, in situ growth, etc., can prepare layered structural composites. Due to the galvanic corrosion between the matrix and Gr, the corrosion resistance would decrease. The corrosion promotion effect derived from highly conductive Gr or rGO can be eliminated by chemical modification or the direct use of Gr derivatives (represented by GO) to fully exploit the barrier properties of Gr.

Advancement from the laboratory to the pilot scale and industrialization is a long journey requiring long-term experiments to monitor service status in realistic working environments. With continuous improvement in the quality and barrier performance of MMCs reinforced with Gr, we foresee that MMCs reinforced with Gr will be widely applied in the marine environment.

#### 7 Conclusion

The equipment used in the marine environment is highly prone to corrosion. It is necessary to analyze the causes of corrosion, elucidate the corrosion mechanism, and explore the principles. This study analyzes the causes of material corrosion induced by high-temperature, high-humidity, and high-salt factors. Combined with the actual service environment, this study analyzes the complex factors that induce corrosion. With high thermal and chemical stability and excellent resistance to permeation, Gr has made remarkable research progress in metal corrosion protection. This study summarizes the recent progress in Gr-metal corrosion-resistant composites. The optimized characteristics of the corrosion performance of Gr and its derivatives are analyzed. And the corrosion resistance mechanisms of Gr composites in metal materials are discussed in terms of these aspects: small size effect of Gr, sheet structure, water resistance, and electrical conductivity. The application of Gr still faces many challenges, for MMC reinforced with Gr, the dispersion, content, size, arrangement, interface, and conductivity of Gr in the composites are critical factors affecting their anti-corrosion properties. With continuous improvement in the quality and barrier performance of MMCs

reinforced with Gr, we foresee that MMCs reinforced with Gr will be widely applied in the marine environment.

Funding information: The authors state no funding involved.

Author contributions: Investigation: Tao Liu, Weimin Lyu, Zhicheng Li, Shengke Wang, Xing Wang, and Jiaxin Jiang; writing — original draft preparation: Tao Liu; writing — review and editing: Tao Liu, Xing Wang, Jiaxin Jiang, and Xiaosong Jiang; project administration: Xiaosong Jiang. All authors have accepted responsibility for the entire content of this manuscript and approved its submission.

**Conflict of interest:** The authors state no conflict of interest.

#### References

- [1] Han YM, Gallant D, Chen XG. Galvanic corrosion associated with Al- $B_4$ C composites/SS304 and Al- $B_4$ C composites/AA6061 couples in NaCl and  $H_3BO_3$  solutions. Electrochim Acta. 2013;94:134–42. doi: 10.1016/j.electacta.2013.01.115.
- [2] Francis R, Hebdon S. The corrosion of cast duplex stainless steels in seawater and sour brines. Corrosion. 2019;75(11):1383–90. doi: 10.5006/3284.
- [3] Yang Y, Zeng H, Xin S, Hou X, Li M. Electrochemical corrosion behavior of 2205 duplex stainless steel in hot concentrated seawater under vacuum conditions. Corros Sci. 2020;165:108383. doi: 10.1016/i.corsci.2019.108383.
- [4] IMPACT the International Measures of Prevention, Application, and Economics of Corrosion Technologies study, NACE International, 2016.
- [5] Panteleeva M. Effective modern methods of protecting metal road structures from corrosion. IOP Conf Ser Earth Environ Sci. 2017;90(1):012119. doi: 10.1088/1755-1315/90/1/012119.
- [6] Li YL, Wang WX, Chen HS, Zhou J, Wu QC. Corrosion behavior of B<sub>4</sub>C/6061Al neutron absorber composite in different H<sub>3</sub>BO<sub>3</sub> concentration solutions. Acta Metall Sin-Engl. 2016;29(11):1037–46. doi: 10.1007/s40195-016-0474-2.
- [7] Winkler SL, Flower HM. Stress corrosion cracking of cast 7XXX aluminium fibre reinforced composites. Corros Sci. 2004;46(4):903–15. doi: 10.1016/j.corsci.2003.09.029.
- [8] Shimizu Y, Nishimura T, Matsushima I. Corrosion resistance of Albased metal matrix composites. Mat Sci Eng A-Struct. 1995;198(1–2):113–8. doi: 10.1016/0921-5093(95)80065-3.
- [9] Li Z, Guo Q, Li Z, Fan G, Xiong DB, Su Y, et al. Enhanced mechanical properties of graphene (reduced graphene oxide)/aluminum composites with a bioinspired nanolaminated structure. Nano Lett. 2015;15(12):8077–83. doi: 10.1021/acs.nanolett.5b03492.
- [10] Wang X, Jiang X, Sun H, Zhang Y, Fang Y, Shu R, et al. Microstructure and mechanical properties of bioinspired laminated Al matrix hybrid reinforced with B<sub>4</sub>C and graphene nanoplatelets. Mater Charact. 2022;193:112307. doi: 10.1016/j.matchar. 2022.112307.

- [11] Gao X, Yue H, Guo E, Zhang H, Lin X, Yao L, et al. Preparation and tensile properties of homogeneously dispersed graphene reinforced aluminum matrix composites. Mater Des. 2016;94:54–60. doi: 10.1016/j.matdes.2016.01.034.
- [12] Wang X, Jiang X, Sun H, Zhang Y. Corrosion behaviour of bioinspired laminated Al matrix composite hybrid reinforced with B<sub>4</sub>C and graphene nanoplatelets. Corros Eng Sci Technol. 2023;58(3):1–11.
- [13] Sun W, Wang L, Wu T, Wang M, Yang Z, Pan Y, et al. Inhibiting the corrosion-promotion activity of graphene. Chem Mater. 2015;27(7):2367–73. doi: 10.1021/cm5043099.
- [14] Kumari S, Panigrahi A, Singh SK, Mohapatra M, Khanna AS, Mishra SK, et al. Electrochemical behavior of nanostructured graphene nickel phosphorus composite coating on copper. J Appl Electrochem. 2019;49:1157–66. doi: 10.1007/s10800-019-01333-y.
- [15] Cai S, Chen X, Liu P, Zhou H, Fu S, Xu K, et al. Fabrication of three-dimensional graphene/Cu-Ag composites by in situ chemical vapor deposition and their properties. J Mater Eng Perform. 2020;29(4):2248–55. doi: 10.1007/s11665-020-04794-x.
- [16] Wang X, Zhang L, Zhou X, Wu W, Jie X. Corrosion behavior of Al<sub>2</sub>O<sub>3</sub>-reinforced graphene encapsulated Al composite coating fabricated by low pressure cold spraying. Surf Coat Technol. 2020;386:125486. doi: 10.1016/j.surfcoat.2020.125486.
- [17] Xie Y, Meng X, Mao D, Qin Z, Wan L, Huang Y. Homogeneously dispersed graphene nanoplatelets as long-term corrosion inhibitors for aluminum matrix composites. Acs Appl Mater Interface. 2021;13(27):32161–74. doi: 10.1021/acsami.1c07148.
- [18] Xia DH, Qin Z, Song S, Macdonald D, Luo JL. Combating marine corrosion on engineered oxide surface by repelling, blocking and capturing Cl<sup>-</sup>: A mini review. Corros Commun. 2021;2:1–7. doi: 10.1016/j.corcom.2021.09.001.
- [19] Li H, Yu H, Zhou T, Yin B, Yin S, Zhang Y. Effect of tin on the corrosion behavior of sea-water corrosion-resisting steel. Mater Des. 2015;84:1–9. doi: 10.1016/j.matdes.2015.06.121.
- [20] Zhao T, Liu Z, Du C, Dai C, Li X, Zhang B. Corrosion fatigue crack initiation and initial propagation mechanism of E690 steel in simulated seawater. Mat Sci Eng A-Struct. 2017;708:181–92. doi: 10.1016/j.msea.2017.09.078.
- [21] Wan S, Wang H, Xia Y, Tieu AK, Tan BH, Zhu H, et al. Investigating the corrosion-fatigue wear on CrN coated piston rings from laboratory wear tests and field trial studies. Wear. 2019;432–433:202940. doi: 10.1016/j.wear.2019.202940.
- [22] Olugbade TO, Ojo OT, Omiyale BO, Olutomilola EO, Olorunfemi BJ. A review on the corrosion fatigue strength of surface-modified stainless steels. J Braz Soc Mech Sci. 2021;43(9):421. doi: 10.1007/s40430-021-03148-5.
- [23] Neville A, Hodgkiess T. An assessment of the corrosion behaviour of high-grade alloys in seawater at elevated temperature and under a high velocity impinging flow. Corros Sci. 1996;38(6):927–56. doi: 10.1016/0010-938x(96)00180-1.
- [24] Pinto GM, Nayak J, Shetty AN. Corrosion behaviour of 6061 Al-15vol. Pct. SiC composite and its base alloy in a mixture of 1:1 hydrochloric and sulphuric acid medium. Int J Electrochem Sci. 2009;4(10):1452–68.
- [25] Zakaria HM. Microstructural and corrosion behavior of Al/SiC metal matrix composites. Ain Shams Eng J. 2014;5(3):831–8. doi: 10.1016/j.asej.2014.03.003.
- [26] Zhang Z, Xu Z, Sung J, Zhu M, Yao Q, Zhang D, et al. Corrosion behaviors of AA5083 and AA6061 in artificial seawater: Effects of

- Cl<sup>-</sup>, HSO<sub>3</sub><sup>-</sup> and temperature. Int J Electrochem Sci. 2020;15(2):1218–29. doi: 10.20964/2020.02.01.
- [27] Zhang Y, Yuan X, Huang H, Zuo X, Cheng Y. Influence of chloride ion concentration and temperature on the corrosion of Cu-Al composite plates in salt fog. J Alloy Compd. 2020;821:153249. doi: 10.1016/j.jallcom.2019.153249.
- [28] Flores JF, Neville A, Kapur N, Gnanavelu A. Corrosion and erosion-corrosion processes of metal-matrix composites in slurry conditions. J Mater Eng Perform. 2012;21(3):395–405. doi: 10.1007/s11665-011-9926-z.
- [29] Padovani C, Winsley RJ, Smart NR, Fennell PAH, Harris C, Christie K. Corrosion control of stainless steels in indoor atmospheres-practical experience (Part 2). Corrosion. 2015;71(5):646–66. doi: 10.5006/1438.
- [30] Schindelholz E, Risteen BE, Kelly RG. Effect of relative humidity on corrosion of steel under sea salt aerosol proxies. J Electrochem Soc. 2014;161(10):C450–9. doi: 10.1149/2.0221410jes.
- [31] Yu Q, Huang YL, Zheng C. Hydrogen permeation and corrosion behaviour of high strength steel 35CrMo under cyclic wet-dry conditions. Corros Eng Sci Technol. 2008;43(3):241–7. doi: 10.1179/ 174327808x286473.
- [32] Liu Y, Wang Z, Wei Y. Influence of seawater on the carbon steel initial corrosion behavior. Int J Electrochem Sci. 2019;14(2):1147–62. doi: 10.20964/2019.02.36.
- [33] Liu J, Li Z, Li Y, Hou B. Corrosion process of D32 steel used for offshore oil platform in splash zone. Anti-Corros Method Mater. 2016;63(1):56–64. doi: 10.1108/acmm-06-2014-1396.
- [34] Zeng J, Zhang G, Long S, Liu K, Cao L, Bao L, et al. Sea salt deliquescence and crystallization in atmosphere: an *in situ* investigation using x-ray phase contrast imaging. Surf Interface Anal. 2013;45(5):930–6. doi: 10.1002/sia.5184.
- [35] Cheng Q, Song S, Song L, Hou B. Effect of relative humidity on the initial atmospheric corrosion behavior of zinc during drying. J Electrochem Soc. 2013;160(8):C380–9. doi: 10.1149/2.078308jes.
- [36] Huang H, Dong Z, Chen Z, Guo X. The effects of Cl<sup>-</sup> ion concentration and relative humidity on atmospheric corrosion behaviour of PCB-Cu under adsorbed thin electrolyte layer. Corros Sci. 2011;53(4):1230–6. doi: 10.1016/j.corsci.2010.12.018.
- [37] Wang P, Zhang D, Qiu R, Wu J, Wan Y. Super-hydrophobic film prepared on zinc and its effect on corrosion in simulated marine atmosphere. Corros Sci. 2013;69:23–30. doi: 10.1016/j.corsci.2012. 10.025
- [38] Hou X, Gao L, Cui Z, Yin J. editors. Iop Corrosion and protection of metal in the seawater desalination. 3rd International Conference on Environmental Science and Material Application (ESMA). Chongging, Peoples R China 2018: 2017 2018 Nov 25–26.
- [39] Alcantara J, de la Fuente D, Chico B, Simancas J, Diaz I, Morcillo M. Marine atmospheric corrosion of carbon steel: A review. Materials. 2017;10(4):406. doi: 10.3390/ma10040406.
- [40] Ambler HR, Bain AAJ. Corrosion of metals in the tropics. J Appl Chem. 1955;5(9):437–67. doi: 10.1002/jctb.5010050901.
- [41] Frankel GS. Pitting corrosion of metals: A review of the critical factors. J Electrochem Soc. 1998;145(6):2186–98. doi: 10.1149/1. 1838615
- [42] Li S, Song J, Wei H, Du H, Wei Y, Hou L. Corrosion behavior of Cu-Ti alloy in simulated S<sup>2-</sup> contaminated seawater. Rare Met Mater Eng. 2022;51(3):895–905.
- [43] Xavier JR. Galvanic corrosion of copper/titanium in aircraft structures using a cyclic wet/dry corrosion test in marine

- environment by EIS and SECM techniques. Sn Appl Sci. 2020;2(8):1-10. doi: 10.1007/s42452-020-3145-x.
- [44] Chen M, Pang K, Liu Z, Wu J, Li X. Influence of rust permeability on corrosion of E690 steel in industrial and non-industrial marine splash zones. J Mater Eng Perform. 2018;27(7):3742-9. doi: 10. 1007/s11665-018-3406-7.
- Liang M, Melchers R, Chaves I. Corrosion and pitting of 6060 series aluminium after 2 years exposure in seawater splash, tidal and immersion zones. Corros Sci. 2018;140:286-96. doi: 10.1016/j. corsci.2018.05.036.
- [46] Bailey SI, Li X, editors. Corrosion of stainless steels in the marine splash zone. 2nd International Conference on Energy, Environment and Sustainable Development (EESD 2012). Jilin, Peoples R China 2013: 2012 2013 Oct 12-14.
- [47] Moradi M, Ye S, Song Z. Dual role of Pseudoalteromonas piscicida biofilm for the corrosion and inhibition of carbon steel in artificial seawater. Corros Sci. 2019;152:10-9. doi: 10.1016/j.corsci.2019. 02.025.
- [48] Lin H, Frankel GS. Atmospheric corrosion of Cu during constant deposition of NaCl. J Electrochem Soc. 2013;160(11):X15-X. doi: 10. 1149/2.030311jes
- [49] Xu Y, Schoonen MAA. The absolute energy positions of conduction and valence bands of selected semiconducting minerals. Am Miner. 2000;85(3-4):543-56. doi: 10.2138/am-2000-0416.
- [50] Moussa SO, Hocking MG. The photo-inhibition of localized corrosion of 304 stainless steel in sodium chloride environment. Corros Sci. 2001;43(11):2037-47. doi: 10.1016/s0010-938x(01)
- Song S, Chen Z. Effect of UV illumination on the NaCl-induced [51] atmospheric corrosion of pure zinc. J Electrochem Soc. 2014;161(6):C288-93. doi: 10.1149/2.015406jes.
- Chen ZY, Liang D, Ma G, Frankel GS, Allen HC, Kelly RG. Influence of UV irradiation and ozone on atmospheric corrosion of bare silver. Corros Eng Sci Technol. 2010;45(2):169-80. doi: 10.1179/ 147842209x12579401586681.
- [53] Li Q, Li W, An M. Sunlight induced photoelectrochemical anticorrosion effect of corrosion product layers on electrogalvanized steel in simulated seawater. Electrochem Commun. 2018;90:39-42. doi: 10.1016/j.elecom.2018.03.010.
- Song L, Ma X, Chen Z, Hou B. The role of UV illumination on the initial atmospheric corrosion of 09CuPCrNi weathering steel in the presence of NaCl particles. Corros Sci. 2014;87:427-37. doi: 10.1016/j.corsci.2014.07.013.
- Li Y, Ning C. Latest research progress of marine microbiological corrosion and bio-fouling, and new approaches of marine anticorrosion and anti-fouling. Bioact Mater. 2019;4:189-95. doi: 10.1016/j.bioactmat.2019.04.003.
- [56] Ma Y, Zhang Y, Zhang R, Guan F, Hou B, Duan J. Microbiologically influenced corrosion of marine steels within the interaction between steel and biofilms: a brief view. Appl Microbiol Biotechnol. 2020;104(2):515-25. doi: 10.1007/s00253-019-10184-8.
- [57] Xu FL, Duan JZ, Lin CG, Hou BR. Influence of marine aerobic biofilms on corrosion of 316L stainless steel. | Iron Steel Res Int. 2015;22(8):715-20. doi: 10.1016/s1006-706x(15)30062-5.
- [58] Rashad M, Pan F, Asif M, Chen X. Corrosion behavior of magnesium-graphene composites in sodium chloride solutions. J Magnes Alloy. 2017;5(3):271-6. doi: 10.1016/j.jma.2017.06.003.
- Itsumi Y, Ellis DE. Electronic bonding characteristics of hydrogen in bcc iron:Part I. Interstitials. J Mater Res. 1996;11:2206. doi: 10. 1557/JMR.1996.0280.

- [60] Krasko GL, Olson GB. Effect of hydrogen on the electronic structure of a grain boundary in iron solid. State Commun. 1991;79:113. doi: 10.1016/0038-1098(91)90072-4.
- [61] Liu X, Zeng D, Wu Y, Zheng Z, Qiu Z. Microstructure and corrosion behavior of HVAF-sprayed Fe-based composite coatings doped TiB<sub>2</sub> and CNTs. Corros Sci. 2022;208:110629. doi: 10.1016/j.corsci.
- Cano H, Diaz I, de la Fuente D, Chico B, Morcillo M. Effect of Cu, Cr [62] and Ni alloying elements on mechanical properties and atmospheric corrosion resistance of weathering steels in marine atmospheres of different aggressivities. Mater Corros. 2018;69(1):8-19. doi: 10.1002/maco.201709656.
- [63] Sun M, Pang Y, Du C, Li X, Wu Y. Optimization of Mo on the corrosion resistance of Cr-advanced weathering steel designed for tropical marine atmosphere. Constr Build Mater. 2021;302:124346. doi: 10.1016/j.conbuildmat.2021.124346.
- Chen X, Liao D, Zhang D, Jiang X, Zhao P, Xu R. Effect of content of [64] graphene on corrosion behavior of micro-arc oxidation coating on titanium alloy drill pipe. Int J Electrochem Sci. 2020;15(1):710-21. doi: 10.20964/2020.01.48.
- Szklarska-Smialowska Z. Pitting corrosion of aluminum. Corros [65] Sci. 1999;41(9):1743-67. doi: 10.1016/s0010-938x(99)00012-8.
- [66] Ao M, Liu H, Dong C, Feng S, Liu J. Degradation mechanism of 6063 aluminium matrix composite reinforced with TiC and Al<sub>2</sub>O<sub>3</sub> particles. J Alloy Compd. 2021;859:157838. doi: 10.1016/j.jallcom.
- [67] Boag A, Taylor RJ, Muster TH, Goodman N, McCulloch D, Ryan C, et al. Stable pit formation on AA2024-T3 in a NaCl environment. Corros Sci. 2010;52(1):90-103. doi: 10.1016/j.corsci. 2009.08.043.
- [68] Huang J, Feng S, Li S, Wu C, Chen J. The crystallographic corrosion and its microstructure in an Al-Cu-Li alloy. J Alloy Compd. 2021;861:158588. doi: 10.1016/j.jallcom.2020.158588.
- [69] Zhao K, Liu J-h, Yu M, Li S-m. Through-thickness inhomogeneity of precipitate distribution and pitting corrosion behavior of Al-Li alloy thick plate. T Nonferr Met Soc. 2019;29(9):1793-802. doi: 10.1016/s1003-6326(19)65087-9.
- [70] Pardo A, Merino MC, Merino S, Viejo F, Carboneras M, Arrabal R. Influence of reinforcement proportion and matrix composition on pitting corrosion behaviour of cast aluminium matrix composites (A3xx.x/SiCp). Corros Sci. 2005;47(7):1750-64. doi: 10.1016/ j.corsci.2004.08.010.
- [71] Hu L, Liu X, Liang C, Zhao S, Chen T, Li J, et al. Microstructure evolution and corrosion mechanism of laser cladded Zr-Cu-Ni-Al in-situ metallic glass matrix composite coatings. Surf Coat Technol. 2021;409:126908. doi: 10.1016/j.surfcoat.2021.126908.
- [72] Yang YJ, Fan XD, Wang FL, Qi HN, Yue Y, Ma MZ, et al. Effect of Nb content on corrosion behavior of Ti-based bulk metallic glass composites in different solutions. Appl Surf Sci. 2019;471:108-17. doi: 10.1016/j.apsusc.2018.11.190.
- Lu L, Wang J, Zheng H, Zhao D, Wang R, Gui J. Spontaneous [73] formation of filamentary Cd whiskers and degradation of CdMqYb icosahedral quasicrystal under ambient conditions. J Mater Res. 2012;27(14):1895-904. doi: 10.1557/jmr.2012.136.
- [74] Ao Y, Ao J, Yang X, Zhao L, Hu L, Le G, et al. Preparation and characterization of hierarchical nanostructures composed by CuO nanowires within directional microporous Cu. Vacuum. 2020;182:109774. doi: 10.1016/j.vacuum.2020.109774.
- [75] Mondal K, Murty BS, Chatterjee UK. Electrochemical behavior of multicomponent amorphous and nanocrystalline Zr-based alloys

- in different environments. Corros Sci. 2006;48(8):2212–25. doi: 10.1016/j.corsci.2005.09.001.
- [76] Al Saadi S, Yi Y, Cho P, Jang C, Beeley P. Passivity breakdown of 316L stainless steel during potentiodynamic polarization in NaCl solution. Corros Sci. 2016;111:720–7. doi: 10.1016/j.corsci.2016. 06.011.
- [77] Burstein GT, Liu C, Souto RM, Vines SP. Origins of pitting corrosion. Corros Eng Sci Technol. 2004;39(1):25–30. doi: 10.1179/147842204225016859v
- [78] Zhou Y, Yan FA. The relation between intergranular corrosion and electrochemical characteristic of carbon steel in carbonic acid and sodium nitrite solutions. Int J Electrochem Sci. 2016;11(5):3976–86.
- [79] Kim HP, Kim DJ. Intergranular corrosion of stainless steel. Corros Sci Technol. 2018;17(4):183–92. doi: 10.14773/cst.2018.17.4.183.
- [80] Liu X, Zhang D, Wang C, Wang X, Zhao Z, Wu M, et al. Effect of grain boundary precipitation on corrosion of heating-aging treated Al-4.47Zn-2.13Mg-1.20Cu alloy. J Mater Res Technol. 2020;9(3):5815–26. doi: 10.1016/j.jmrt.2020.03.106.
- [81] Ralston KD, Birbilis N. Effect of Grain Size on Corrosion: A Review. Corrosion. 2010;66(7):075005. doi: 10.5006/1.3462912.
- [82] Ralston KD, Fabijanic D, Birbilis N. Effect of grain size on corrosion of high purity aluminium. Electrochim Acta. 2011;56(4):1729–36. doi: 10.1016/j.electacta.2010.09.023.
- [83] Ralston KD, Birbilis N, Davies CHJ. Revealing the relationship between grain size and corrosion rate of metals. Scr Mater. 2010;63(12):1201–4. doi: 10.1016/j.scriptamat.2010.08.035
- [84] Ralston KD, Birbilis N, Cavanaugh MK, Weyland M, Muddle BC, Marceau RKW. Role of nanostructure in pitting of Al-Cu-Mg alloys. Electrochim Acta. 2010;55(27):7834–42. doi: 10.1016/j.electacta. 2010.02.001.
- [85] Burleigh TD. The postulated mechanisms for stress-corrosion cracking of aluminum-alloys - A review of the literature 1980-1989. Corrosion. 1991;47(2):89–98. doi: 10.5006/1.3585235.
- [86] Holroyd NJH, Vasudevan AK, Christodoulou L. Stress corrosion of high-strength aluminium alloys. Treatise Mater Sci Technol. 1989;31:463–83. doi: 10.1016/B978-0-12-341831-9.50021-8.
- [87] Liu G, Geng J, Li Y, Li H, Wang M, Chen D, et al. Improved stress corrosion cracking resistance of in-situ TiB<sub>2</sub>/7050Al composite by pre-precipitation treatment. Micron. 2021;145:103056. doi: 10. 1016/j.micron.2021.103056.
- [88] Bunch JS, Verbridge SS, Alden JS, van der Zande AM, Parpia JM, Craighead HG, et al. Impermeable atomic membranes from graphene sheets. Nano Lett. 2008;8(8):2458–62. doi: 10.1021/ nl801457b.
- [89] Topsakal M, Şahin H, Ciraci S. Graphene coatings: an efficient protection from oxidation. Phys Rev B. 2012;85(15):155445. doi: 10.1103/PhysRevB.85.155445.
- [90] Zhang R, Yu X, Yang Q, Cui G, Li Z. The role of graphene in anticorrosion coatings: A review. Constr Build Mater. 2021;294:123613. doi: 10.1016/j.conbuildmat.2021.123613.
- [91] Kong W, Kum H, Bae S-H, Shim J, Kim H, Kong L, et al. Path towards graphene commercialization from lab to market. Nat Nanotechnol. 2019;14(10):927–38. doi: 10.1038/s41565-019-0555-2.
- [92] Vashist SK, Luong JHT. Recent advances in electrochemical biosensing schemes using graphene and graphene-based nano-composites. Carbon. 2015;84:519–50. doi: 10.1016/j.carbon.2014. 12.052.
- [93] Raman RKS, Banerjee PC, Lobo DE, Gullapalli H, Sumandasa M, Kumar A, et al. Protecting copper from electrochemical

- degradation by graphene coating. Carbon. 2012;50(11):4040–5. doi: 10.1016/j.carbon.2012.04.048.
- [94] Pingale AD, Belgamwar SU, Rathore JS. Effect of graphene nanoplatelets addition on the mechanical, tribological and corrosion properties of Cu-Ni/Gr nanocomposite coatings by electroco-deposition method. T Indian I Met. 2020;73(1):99-107. doi: 10.1007/s12666-019-01807-9.
- [95] Behera AK, Patel AK, Mehta R, Sarkar S, Das S, Mallik A. Exploration of in-house synthesized and functionalized graphene as reinforcement in Cu-matrix for improved mechanical and anticorrosion properties. Diam Relat Mater. 2020;109:108009. doi: 10.1016/j.diamond.2020.108009.
- [96] Kakaei K, Esrafili MD, Ehsani A. Graphene and anticorrosive properties. Interface Sci Technol. 2019;27:303–37. doi: 10.1016/ B978-0-12-814523-4.00008-3.
- [97] Camilli L, Yu F, Cassidy A, Hornekaer L, Boggild P. Challenges for continuous graphene as a corrosion barrier. 2D Mater. 2019;6(2):022002. doi: 10.1088/2053-1583/ab04d4.
- [98] Ding R, Chen S, Lv J, Zhang W, Zhao XD, Liu J, et al. Study on graphene modified organic anti-corrosion coatings: A comprehensive review. J Alloy Compd. 2019;806:611–35. doi: 10.1016/j. jallcom.2019.07.256.
- [99] Jiang S, Liu Z, Jiang D, Cheng H, Han J, Han S. Graphene as a nanotemplating auxiliary on the polypyrrole pigment for anticorrosion coatings. High Perform Polym. 2016;28(6):747–57. doi: 10.1177/0954008316647469.
- [100] Huh JH, Kim SH, Chu JH, Kim SY, Kim JH, Kwon SY. Enhancement of seawater corrosion resistance in copper using acetone-derived graphene coating. Nanoscale. 2014;6(8):4379–86. doi: 10.1039/ c3nr05997a.
- [101] Xu X, Yi D, Wang Z, Yu J, Zhang Z, Qiao R, et al. Greatly Enhanced Anticorrosion of Cu by Commensurate Graphene Coating. Adv Mater. 2018;30(6):170294. doi: 10.1002/adma.201702944.
- [102] Zhu YX, Duan CY, Liu HY, Chen YF, Wang Y. Graphene coating for anti-corrosion and the investigation of failure mechanism. J Phys D Appl Phys. 2017;50(11):114001. doi: 10.1088/1361-6463/aa5bb0.
- [103] Wu Y, Yu J, Zhao W, Wu W, Dong J, Zhou K, et al. Excellent corrosion resistance of graphene coating on copper due to the low defect overlapping structure. Surf Topogr-Metrol. 2019;7(1):015014. doi: 10.1088/2051-672X/ab030f.
- [104] Morales-Narvaez E, Florio Sgobbi L, Spinola Machado SA, Merkoci A. Graphene-encapsulated materials: Synthesis, applications and trends. Prog Mater Sci. 2017;86:1–24. doi: 10.1016/j. pmatsci.2017.01.001.
- [105] Ahmad H, Fan M, Hui D. Graphene oxide incorporated functional materials: A review. Compos Part B-Eng. 2018;145:270–80. doi: 10.1016/j.compositesb.2018.02.006.
- [106] Zhang H, Wang S, Lin Y, Feng M, Wu Q. Stability, thermal conductivity, and rheological properties of controlled reduced graphene oxide dispersed nanofluids. Appl Therm Eng. 2017;119:132–9. doi: 10.1016/j.applthermaleng.2017.03.064.
- [107] He Y, Wang S, Luo H, Wang C. Ag-rGO content dependence of the mechanical, conductive and anti-corrosion properties of copper matrix composites. Mater Res Express. 2018;5(9):096523. doi: 10. 1088/2053-1591/aad8e7.
- [108] Hayatgheib Y, Ramezanzadeh B, Kardar P, Mandavian M. A comparative study on fabrication of a highly effective corrosion protective system based on graphene oxide-polyaniline nanofibers/epoxy composite. Corros Sci. 2018;133:358–73. doi: 10.1016/j. corsci.2018.01.046.

- Cui C, Lim ATO, Huang J. A cautionary note on graphene anticorrosion coatings. Nat Nanotechnol. 2017;12:834-5. doi: 10.1038/ nnano.2017.187.
- [110] Ramezanzadeh B, Ghasemi E, Mahdavian M, Changizi E, Moghadam MHM. Covalently-grafted graphene oxide nanosheets to improve barrier and corrosion protection properties of polyurethane coatings. Carbon. 2015;93:555-73. doi: 10.1016/j.carbon.2015.05.094.
- Sun W, Wu T, Wang L, Yang Z, Zhu T, Dong C, et al. The role of graphene loading on the corrosion-promotion activity of graphene/epoxy nanocomposite coatings. Compos Part B-Eng. 2019;173:106916. doi: 10.1016/j.compositesb.2019.106916.
- Cui G, Bi Z, Zhang R, Liu J, Yu X, Li Z. A comprehensive review on graphene-based anti-corrosive coatings. Chem Eng J. 2019;373:104-21. doi: 10.1016/j.cej.2019.05.034.
- [113] Huang YC, Lo TY, Chao CG, Whang WT. Anti-corrosion characteristics of polyimide/h-boron nitride composite films with different polymer configurations. Surf Coat Technol. 2014;260:113-7. doi: 10.1016/j.surfcoat.2014.09.043.
- [114] Shen L, Zhao Y, Wang Y, Song R, Yao Q, Chen S, et al. A long-term corrosion barrier with an insulating boron nitride monolayer. J Mater Chem A. 2016;4(14):5044-50. doi: 10.1039/c6ta01604a.
- [115] Mahvash F, Eissa S, Bordjiba T, Tavares AC, Szkopek T, Siaj M. Corrosion resistance of monolayer hexagonal boron nitride on copper. Sci Rep-Uk. 2017;7:42139. doi: 10.1038/srep42139.
- Zhao H, Ding J, Yu H. The efficient exfoliation and dispersion of hBN nanoplatelets: advanced application to waterborne anticorrosion coatings. N J Chem. 2018;42(17):14433-43. doi: 10.1039/ c8nj03113d.
- [117] Zhang Y, Tian J, Zhong J, Shi X. Thin nacre-biomimetic coating with super-anticorrosion performance. ACS Nano. 2018;12(10):10189-200. doi: 10.1021/acsnano.8b05183.
- [118] Kumari S, Panigrahi A, Singh SK, Pradhan SK. Enhanced corrosion resistance and mechanical properties of nanostructured graphene-polymer composite coating on copper by electrophoretic deposition. J Coat Technol Res. 2018;15(3):583-92. doi: 10.1007/ s11998-017-0001-z.
- Pourhashem S, Ghasemy E, Rashidi A, Vaezi MR. Corrosion protection properties of novel epoxy nanocomposite coatings containing silane functionalized graphene quantum dots. J Alloy Compd. 2018;731:1112-8. doi: 10.1016/j.jallcom.2017.10.150.
- [120] Kumar CMP, Venkatesha TV, Shabadi R. Preparation and corrosion behavior of Ni and Ni-graphene composite coatings. Mater Res Bull. 2013;48(4):1477-83. doi: 10.1016/j.materresbull.2012. 12.064.
- [121] Szeptycka B, Gajewska-Midzialek A, Babul T. Electrodeposition and corrosion resistance of Ni-graphene composite coatings. J Mater Eng Perform. 2016;25(8):3134-8. doi: 10.1007/s11665-016-2009-4.
- [122] Zhang R, Cui G, Su X, Yu X, Li Z. A novel functionally graded Ni-graphene coating and its corrosion resistance. J Alloy Compd. 2020;829:154495. doi: 10.1016/j.jallcom.2020.154495.
- Qin BD, Ma LQ, Wang SC, Hou CJ, Zhou SG. Construction of a [123] sandwich-like Gr/Ni composite coating on AZ91D magnesium alloy to achieve excellent corrosion and wear resistances in the seawater. Diam Relat Mater. 2022;130:109400. doi: 10.1016/j. diamond.2022.109400.
- [124] Askarnia R, Ghasemi B, Fardi SR, Adabifiroozjaei E. Improvement of tribological, mechanical and chemical properties of Mg alloy (AZ91D) by electrophoretic deposition of alumina/GO coating.

- Surf Coat Technol. 2020;403:126410. doi: 10.1016/j.surfcoat.2020.
- [125] Rekha MY, Srivastava C. Microstructure and corrosion properties of zinc-graphene oxide composite coatings. Corros Sci. 2019;152:234-48. doi: 10.1016/j.corsci.2019.03.015.
- [126] Yolshina LA, Muradymov RV, Molchanova NG. Corrosion behavior of aluminum-graphene and aluminum-graphite composite materials in a 3% NaCl aqueous solution. Russ Metall+. 2022;2022(2):153-60. doi: 10.1134/s0036029522020057.
- [127] Selvam M, Saminathan K, Siva P, Saha P, Rajendran V. Corrosion behavior of Mg/graphene composite in aqueous electrolyte. Mater Chem Phys. 2016;172:129-36. doi: 10.1016/j.matchemphys.
- [128] Turan ME, Sun Y, Akgul Y, Turen Y, Ahlatci H. The effect of GNPs on wear and corrosion behaviors of pure magnesium. I Alloy Compd. 2017;724:14-23. doi: 10.1016/j.jallcom.2017.07.022.
- Wang J, Guo LN, Lin WM, Chen J, Zhang S, Chen SD, et al. The [129] effects of graphene content on the corrosion resistance, and electrical, thermal and mechanical properties of graphene/ copper composites. Carbon. 2019;150:551. doi: 10.1016/j.carbon. 2019.04.095.
- [130] AbuShanab WS, Moustafa EB, Ghandourah E, Taha MA. Effect of graphene nanoparticles on the physical and mechanical properties of the Al2024-graphene nanocomposites fabricated by powder metallurgy. Results Phys. 2020;19:103343. doi: 10.1016/j. rinp.2020.103343.
- [131] Cui M, Ren S, Zhao H, Xue Q, Wang L. Polydopamine coated graphene oxide for anticorrosive reinforcement of water-borne epoxy coating. Chem Eng J. 2018;335:255-66. doi: 10.1016/j.cej. 2017.10.172.
- [132] Gao XZ, Liu HJ, Cheng F, Chen Y. Thermoresponsive polyaniline nanoparticles: Preparation, characterization, and their potential application in waterborne anticorrosion coatings. Chem Eng J. 2016;283:682-91. doi: 10.1016/j.cej.2015.08.015.
- [133] Li Y, Yang Z, Qiu H, Dai Y, Zheng Q, Li J, et al. Self-aligned graphene as anticorrosive barrier in waterborne polyurethane composite coatings. J Mater Chem A. 2014;2(34):14139-45. doi: 10.1039/c4ta02262a.
- [134] Ding R, Chen S, Lv J, Gui TJ, Wang X, Zhao XD, et al. Review of theoretical and applied research of graphene in anti-corrosion film and organic anti-corrosion coatings. Acta Chim Sin. 2019;77(11):1140-55. doi: 10.6023/a19050174.
- [135] Pang H, Chen C, Zhang YC, Ren PG, Yan DX, Li ZM. The effect of electric field, annealing temperature and filler loading on the percolation threshold of polystyrene containing carbon nanotubes and graphene nanosheets. Carbon. 2011;49(6):1980-8. doi: 10.1016/j.carbon.2011.01.023.
- [136] Zhao X, Zhang Q, Hao Y, Li Y, Fang Y, Chen D. Alternate multilayer films of poly(vinyl alcohol) and exfoliated graphene oxide fabricated via a facial layer-by-layer assembly. Macromolecules. 2010;43(22):9411-6. doi: 10.1021/ma101456y.
- [137] Xu H, Zang J, Yuan Y, Tian P, Wang Y. Fabrication of graphene coating bonded to mild steel via covalent bonding for high anticorrosion performance. J Alloy Compd. 2019;805:967-76. doi: 10.1016/j.jallcom.2019.07.159.
- [138] Uzoma PC, Liu F, Xu L, Zhang Z, Han EH, Ke W, et al. Superhydrophobicity, conductivity and anticorrosion of robust siloxane-acrylic coatings modified with graphene nanosheets. Prog Org Coat. 2019;127:239-51. doi: 10.1016/j.porgcoat.2018. 11.018.

- [139] Chen Z, Hou C, Zhang Q, Li Y, Wang H. Reinforced heat dissipation by simple graphene coating for phosphor-in-glass applied in high-power LED. J Alloy Compd. 2019;774:954–61. doi: 10.1016/j. jallcom.2018.09.395.
- [140] Cheng L, Liu C, Han D, Ma S, Guo W, Cai H, et al. Effect of graphene on corrosion resistance of waterborne inorganic zincrich coatings. J Alloy Compd. 2019;774:255–64. doi: 10.1016/j. iallcom.2018.09.315.
- [141] Tang X, Zhou Y, Peng M. Green preparation of epoxy/graphene oxide nanocomposites using a glycidylamine epoxy resin as the surface modifier and phase transfer agent of graphene oxide. ACS Appl Mater Interface. 2015;8:1854–66. doi: 10.1021/acsami. 5h09830
- [142] Boehm S. Graphene against corrosion. Nat Nanotechnol. 2014;9(10):741–2. doi: 10.1038/nnano.2014.220.
- [143] Wang B, Cunning BV, Park S-Y, Huang M, Kim J-Y, Ruoff RS. Graphene coatings as barrier layers to prevent the water-induced corrosion of silicate glass. ACS Nano. 2016;10(11):9794–800. doi: 10.1021/acsnano.6b04363.
- [144] Prasai D, Tuberquia JC, Harl RR, Jennings GK, Bolotin KI. Graphene: corrosion-inhibiting coating. ACS Nano. 2012;6(2):1102–8. doi: 10.1021/nn203507y.
- [145] Schriver M, Regan W, Gannett WJ, Zaniewski AM, Crommie MF, Zettl A. Graphene as a long-term metal oxidation barrier: worse than nothing. ACS Nano. 2013;7(7):5763–8. doi: 10.1021/ nn4014356
- [146] Ren S, Cui M, Li W, Pu J, Xue Q, Wang L. N-doping of graphene: toward long- term corrosion protection of Cu. J Mater Chem A. 2018;6(47):24136–48. doi: 10.1039/c8ta05421e.
- [147] Chang CH, Huang TC, Peng CW, Yeh TC, Lu HI, Hung WI, et al. Novel anticorrosion coatings prepared from polyaniline/graphene composites. Carbon. 2012;50(14):5044–51. doi: 10.1016/j. carbon.2012.06.043.
- [148] Roding M, Gaska K, Kadar R, Loren N. Computational screening of diffusive transport in nanoplatelet-filled composites: Use of graphene to enhance polymer barrier properties. ACS Appl Nano Mater. 2018;1(1):160–7. doi: 10.1021/acsanm.7b00067.
- [149] Khodabakhshi F, Arab SM, Svec P, Gerlich AP. Fabrication of a new Al-Mg/graphene nanocomposite by multi-pass friction-stir processing: Dispersion, microstructure, stability, and strengthening. Mater Charact. 2017;132:92–107. doi: 10.1016/j.matchar.2017. 08.009.
- [150] Yu M, Shao D, Lu F, Sun X, Sun H, Hu T, et al. ZnO/graphene nanocomposite fabricated by high energy ball milling with

- greatly enhanced lithium storage capability. Electrochem Commun. 2013;34:312–5. doi: 10.1016/j.elecom.2013.07.013.
- [151] He S, Liang J, Yuan J, He J, Hu H, Gao Y. Preparation of graphene dispersing system stabilized by ethanol amine and its pHresponse property. Fine Chem. 2016;33(1):8–13.
- [152] Shuai C, Wang B, Yang Y, Peng S, Gao C. 3D honeycomb nanostructure-encapsulated magnesium alloys with superior corrosion resistance and mechanical properties. Compos Part B-Eng. 2019;162:611–20. doi: 10.1016/j.compositesb.2019.01.031.
- [153] Ramezanzadeh B, Ahmadi A, Mandavian M. Enhancement of the corrosion protection performance and cathodic delamination resistance of epoxy coating through treatment of steel substrate by a novel nanometric sol-gel based silane composite film filled with functionalized graphene oxide nanosheets. Corros Sci. 2016;109:182–205. doi: 10.1016/j.corsci.2016.04.004.
- [154] Jin B, Xiong D-B, Tan Z, Fan G, Guo Q, Su Y, et al. Enhanced corrosion resistance in metal matrix composites assembled from graphene encapsulated copper nanoflakes. Carbon. 2019;142:482–90. doi: 10.1016/j.carbon.2018.10.088.
- [155] Um JG, Jun YS, Alhumade H, Krithivasan H, Lui G, Yu A. Investigation of the size effect of graphene nano-platelets (GnPs) on the anti-corrosion performance of polyurethane/GnP composites. RSC Adv. 2018;8(31):17091–100. doi: 10.1039/C8RA02087F.
- [156] Sun PZ, Yang Q, Kuang WJ, Stebunov YV, Xiong WQ, Yu J, et al. Limits on gas impermeability of graphene. Nature. 2020;579:229–32. doi: 10.1038/s41586-020-2070-x.
- [157] Jiang D, Cooper VR, Dai S. Porous graphene as the ultimate membrane for gas separation. Nano Lett. 2009;9(12):4019–24. doi: 10.1021/nl9021946.
- [158] Grimme S, Antony J, Ehrlich S, Krieg H. A consistent and accurate ab initio parametrization of density functional dispersion correction (DFT-D) for the 94 elements H-Pu. J Chem Phys. 2010;132(15):154104. doi: 10.1063/1.3382344.
- [159] Zhao Y, Liu Z, Sun T, Zhang L, Jie W, Wang X, et al. Mass transport mechanism of Cu species at the metal/dielectric interfaces with a graphene barrier. ACS Nano. 2014;8(12):12601–11. doi: 10.1021/ nn5054987.
- [160] Zhang H, Ren S, Pu J, Xue Q. Barrier mechanism of multilayer graphene coated copper against atomic oxygen irradiation. Appl Surf Sci. 2018;444:28–35. doi: 10.1016/j.apsusc.2018.03.026.
- [161] Tian H, Seh ZW, Yan K, Fu Z, Tang P, Lu Y, et al. Theoretical investigation of 2D layered materials as protective films for lithium and sodium metal anodes. Adv Energy Mater. 2017;7(13):1602528. doi: 10.1002/aenm.201602528.